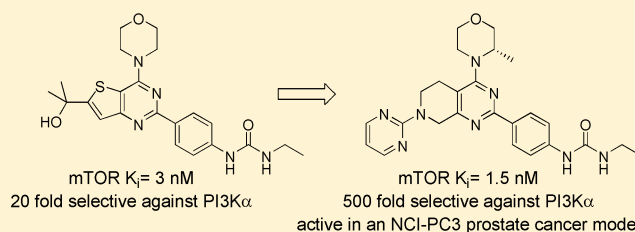


## Potent, Selective, and Orally Bioavailable Inhibitors of the Mammalian Target of Rapamycin Kinase Domain Exhibiting Single Agent Antiproliferative Activity

Michael F. T. Koehler,<sup>\*,†</sup> Philippe Bergeron,<sup>†</sup> Elizabeth Blackwood,<sup>‡</sup> Krista K. Bowman,<sup>§</sup> Yung-Hsiang Chen,<sup>#</sup> Gauri Deshmukh,<sup>#</sup> Xiao Ding,<sup>#</sup> Jennifer Epler,<sup>‡</sup> Kevin Lau,<sup>†</sup> Leslie Lee,<sup>‡</sup> Lichuan Liu,<sup>#</sup> Cuong Ly,<sup>†</sup> Shiva Malek,<sup>‡</sup> Jim Nonomiya,<sup>||</sup> Jason Oeh,<sup>‡</sup> Daniel F. Ortwine,<sup>†</sup> Deepak Sampath,<sup>‡</sup> Steve Sideris,<sup>||</sup> Lan Trinh,<sup>||</sup> Tom Truong,<sup>‡</sup> Jiansheng Wu,<sup>∇</sup> Zhonghua Pei,<sup>†</sup> and Joseph P. Lyssikatos<sup>†</sup>

<sup>†</sup>Department of Discovery Chemistry, <sup>‡</sup>Department of Translational Oncology, <sup>§</sup>Department of Structural Biology, <sup>||</sup>Department of Small Molecule Biochemical Pharmacology, <sup>#</sup>Department of Drug Metabolism and Pharmacokinetics, and <sup>∇</sup>Department of Protein Chemistry, Genentech, Inc., 1 DNA Way, South San Francisco, California 94080, United States

**ABSTRACT:** Selective inhibitors of mammalian target of rapamycin (mTOR) kinase based upon saturated heterocycles fused to a pyrimidine core were designed and synthesized. Each series produced compounds with  $K_i < 10$  nM for the mTOR kinase and >500-fold selectivity over closely related PI3K kinases. This potency translated into strong pathway inhibition, as measured by phosphorylation of mTOR substrate proteins and antiproliferative activity in cell lines with a constitutively active PI3K pathway. Two compounds exhibiting suitable mouse PK were profiled in in vivo tumor models and were shown to suppress mTORC1 and mTORC2 signaling for over 12 h when dosed orally. Both compounds were additionally shown to suppress tumor growth in vivo in a PC3 prostate cancer model over a 14 day study.



## INTRODUCTION

As the role of misregulation of signaling pathways in various cancers has become better understood, activating mutations in the growth factor receptor tyrosine kinase/phosphoinositide 3-kinase (PI3K)/Akt pathway stand out as being implicated in a multitude of cancers. More recent work has shown that the mammalian target of rapamycin (mTOR) serves as an essential component of this signaling pathway. mTOR is a serine-threonine protein kinase of the PI3K superfamily and forms two distinct signaling complexes, mTOR complexes 1 and 2 (mTORC1 and -2).

The mTORC1 complex is known to phosphorylate 4EBP1 and S6K1, thereby stimulating CAP-dependent translation, protein synthesis, and cell proliferation. mTORC2 has been found to phosphorylate and activate Akt upstream of mTORC1. The natural product rapamycin (**1a**) and its semisynthetic analogs temsirolimus (**1b**) and everolimus (**1c**) (Figure 1) are selective allosteric inhibitors of most of the functions of mTORC1 but do not inhibit mTORC2. While everolimus has demonstrated efficacy when combined with exemestane in hormone receptor positive breast cancer,<sup>1</sup> both temsirolimus and everolimus have been shown to have only modest efficacy in treating renal cell carcinoma and mantle cell lymphoma. This limited efficacy has been ascribed to the existence of two feedback pathways, mediated by mTORC2, which induce hyperphosphorylation of Akt in the presence of

rapamycin.<sup>2</sup> These results prompted a great interest in developing inhibitors of the kinase domain of mTOR which would inhibit both mTORC1 and mTORC2, a number of which have been reported recently.<sup>3–28</sup>

## RESULTS AND DISCUSSION

Having previously developed both the PI3K selective<sup>29</sup> compound **2** (GDC-0941, Figure 1) and the potent dual PI3K/mTOR inhibitor<sup>30</sup> **3** (GDC-0980, Figure 1), we focused on producing an inhibitor specific for mTOR that would enable us to assess the role mTOR signaling was playing in various cell lines and cancer types. Our starting point was morpholinopyrimidine **4**, which had been found to be a potent inhibitor of the mTOR kinase with a  $K_i = 3$  nM that was also 20-fold selective for mTOR over PI3K $\alpha$ .

Our initial efforts were directed at moving away from the thienopyrimidine scaffold used in our previous work, which we knew from previous experience could present difficulties with solubility, oral bioavailability, and poor pharmacokinetics.<sup>30</sup> In an effort to improve the predicted solubility, clogP, and predicted metabolic stability of our core, we targeted replacement of the thiophene with a saturated ring. Pyrrolidine was an attractive replacement as it provided a functional handle

Received: September 24, 2012

Published: November 30, 2012

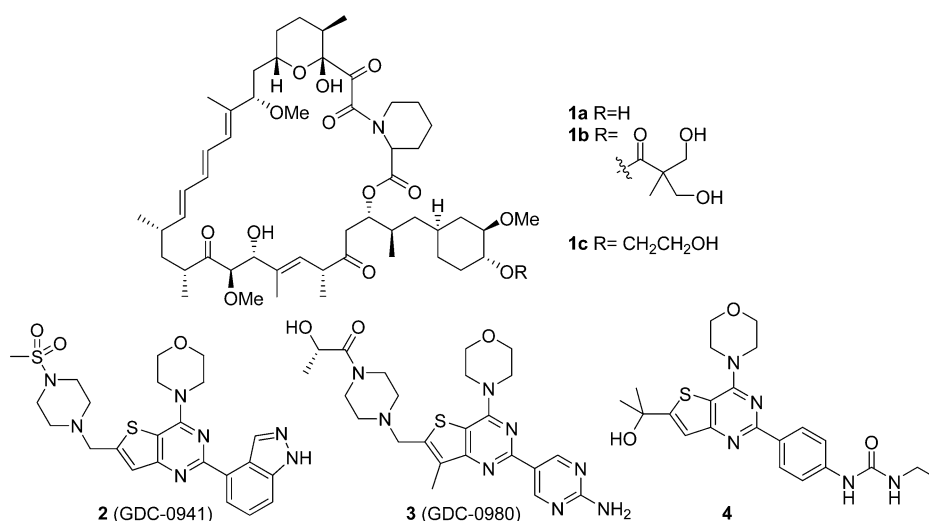
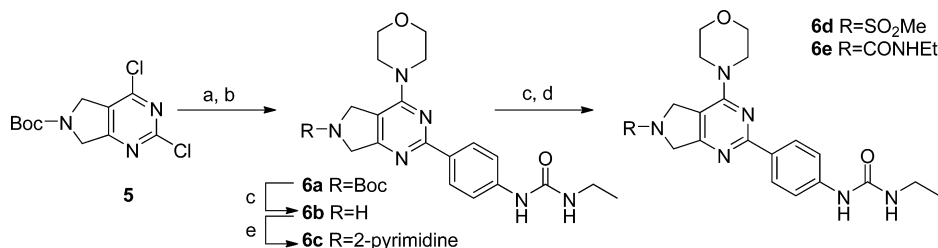


**Figure 1.** Rapamycin and its analogs 1a–c, selective PI3K inhibitor 2 (GDC-0941), dual PI3K/mTOR inhibitor 3 (GDC-0980), and 4, which exhibits 20-fold mTOR selectivity.

### Scheme 1. Synthesis of Pyrrolopyrimidines 6a–e<sup>a</sup>



<sup>a</sup>Reagents and conditions: (a) morpholine, DIPEA, 90%; (b) (4-ethylurido)phenylboronic acid pinacol ester, Pd(PPh<sub>3</sub>)<sub>4</sub>, KOAc, Na<sub>2</sub>CO<sub>3</sub>, H<sub>2</sub>O/CH<sub>3</sub>CN, 120 °C, 96%; (c) TFA, CH<sub>2</sub>Cl<sub>2</sub>, then PS-carbonate resin; (d) electrophile, DIPEA, CH<sub>2</sub>Cl<sub>2</sub>, (e) 2-chloropyrimidine, DIPEA, DMF, 120 °C.

for further diversification after assembly of the core. Molecules of this type could be rapidly assembled from the Boc-2,4-dichloro-5-pyrrolopyrimidine 5 through nucleophilic displacement of the C4 chloride followed by a Suzuki coupling at C2. Potassium acetate was included in the coupling to minimize the cleavage of the ethyl urea, which was a major side product when sodium carbonate was the exclusive base. Final diversification was accomplished by removal of the Boc group followed by treatment with an appropriate electrophile, as shown in Scheme 1.

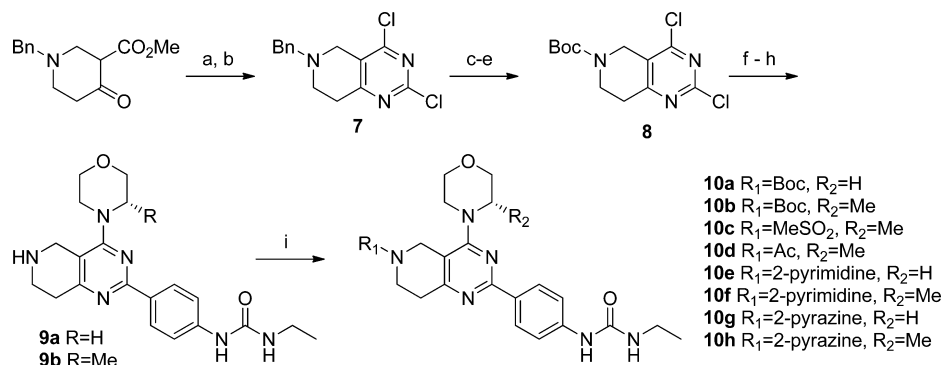
The *in vitro* potencies of these compounds were measured against recombinant mTOR kinase domain using a Lanthascreen FRET assay and against PI3K $\alpha$  using a fluorescence polarization assay, as previously described.<sup>31</sup> PI3K $\alpha$  was chosen as our initial antitarget as a representative class I PI3 kinase. We were pleased to discover that, with the exception of the unsubstituted pyrrolidine, all of these compounds were potent inhibitors of the mTOR kinase domain. Unexpectedly, the compounds also exhibited improved selectivity against PI3K $\alpha$  relative to the starting thienopyrimidine (Table 1). At the same time, we observed chemical instability in a subset of these molecules upon standing in DMSO solution in air. We did not characterize this instability extensively but supposed it stemmed from oxidation of the doubly activated benzylic methylenes. We therefore began investigating alternative saturated ring systems to identify those which would be tolerated in place of the pyrrolidine and would not exhibit this instability.

**Table 1. Inhibition Data for Pyrrolopyrimidines 6a–e<sup>a</sup>**

	R	mTOR K <sub>i</sub> (nM)	PI3K $\alpha$ (fold)
6a	Boc	10	21
6b	H	122	82
6c	2-pyrimidine	3.0	126
6d	SO <sub>2</sub> Me	3.7	82
6e	CONHET	5.1	42

<sup>a</sup>Assays are described in ref 30.

We began by investigating the possibility of expanding the pyrrolidine ring to a piperidine, thereby eliminating one of the doubly activated methylenes. Of the two possibilities, we first examined those in which the nitrogen on the saturated ring was in the 6-position. The synthesis of these compounds proved straightforward (Scheme 2), beginning with the formation of the pyrimidine dione from methyl 1-benzyl-4-oxopiperidine-3-carboxylate. This could be converted to the dichloride 7 and the benzyl protecting group exchanged for Boc using ACE-Cl<sup>32</sup> to give 8. Nucleophilic aromatic substitution with a morpholine followed by Suzuki coupling and Boc removal gave compounds

Scheme 2. Synthesis of 6-Aza-tetrahydroquinazolines 10<sup>a</sup>

<sup>a</sup>Reagents and conditions: (a) urea, MeOH, NaOMe, reflux, 64%; (b) POCl<sub>3</sub>, reflux, 75%; (c) ACE-Cl, CH<sub>2</sub>Cl<sub>2</sub>, 0 °C to rt, then reflux; (d) MeOH, reflux; (e) PS-carbonate resin, Boc<sub>2</sub>O, CH<sub>2</sub>Cl<sub>2</sub>, 88% for three steps; (f) morpholine or (*S*)-methylmorpholine, DIPEA, DMF; (g) (4-ethylurido)phenylboronic acid pinacol ester, Pd(PPh<sub>3</sub>)<sub>4</sub>, KOAc, Na<sub>2</sub>CO<sub>3</sub>, H<sub>2</sub>O/CH<sub>3</sub>CN, 120 °C; (h) TFA, CH<sub>2</sub>Cl<sub>2</sub>, then PS-carbonate resin; (i) electrophile, DIPEA, CH<sub>2</sub>Cl<sub>2</sub>.

**9a** and **9b**, which could be functionalized as needed through acylation, sulfonylation, or nucleophilic aromatic substitution to give the desired 6-aza-tetrahydroquinazolines **10**.

The 6-aza-tetrahydroquinazolines **10a–h** proved to be less potent but more selective inhibitors of mTOR than the equivalent pyrrolopyrimidines **6**, as seen in Table 2. Addition-

**Table 2. Inhibition Data for 6-Aza-tetrahydroquinazoline Compounds 10a–h<sup>a</sup>**

	R <sub>1</sub>	R <sub>2</sub>	mTOR K <sub>i</sub> (nM)	PI3K α/δ (fold)
<b>10a</b>	Boc	H	48	10/48
<b>10b</b>	Boc	Me	12	214/224
<b>10c</b>	MeSO <sub>2</sub>	Me	6.8	>1000/>1000
<b>10d</b>	Ac	Me	11	>900/>900
<b>10e</b>	2-pyrimidine	H	17	120/61
<b>10f</b>	2-pyrimidine	Me	2.3	>900/>900
<b>10g</b>	2-pyrazine	H	20	69/91
<b>10h</b>	2-pyrazine	Me	2.4	>1000/>1000

<sup>a</sup>Assays are described in ref 30.

ally, all proved stable under our typical handling conditions. To investigate the source of the diminished activity, we examined compound **10f** docked into a homology model of mTOR that was built using PI3Kγ as a template (Figure 2). The model indicates that the 6-N-substituents make a close approach to the protein, but are not predicted to make unfavorable interactions. The observed loss of affinity could be partially compensated for by incorporating an (*S*)-2-methylmorpholine, which has been shown to enhance potency and selectivity for mTOR when used in place of morpholine as a hinge binder,<sup>9,21</sup> as this methyl group projects into a hydrophobic cavity created by Trp2239 that PI3Kα lacks. In the examples below, the methyl group improved mTOR potency an average of 6.6-fold,

with an 8.0-fold improvement in selectivity against PI3Kα. Encouraged by the improved selectivity of these compounds for the mTOR kinase, we decided to investigate the isomeric 7-aza-tetrahydroquinazolinone series, as our modeling indicated that substituents on the piperidine nitrogen would be more completely solvent exposed.

We prepared the 7-aza-tetrahydroquinazolines using chemistry analogous to that developed for the synthesis of the pyrrolopyrimidines (Scheme 3). When assayed (Table 3), we found that this series of compounds had recovered the potency and selectivity for mTOR over both PI3Kα and PI3Kδ we had observed in the pyrrolidine series, and all were again found to be stable under typical storage conditions.

Our initial inhibition data indicated that both polar and nonpolar functionality was tolerated on the piperidine nitrogen with little change in the biochemical potency. Docking of these molecules into a homology model of mTOR shows that N-substituents are directed into a largely solvent-exposed region of the protein (Figure 3). The basic piperidine, left unmodified, reduced the potency approximately 10-fold, but reducing the basicity through formation of a carbamate, sulfonamide, urea, or ester resulted in compounds of approximately equivalent K<sub>i</sub>. Modeling shows this nitrogen is in a fairly hydrophobic region of the protein, flanked by Ile2163, Leu2185, Trp2239, Met2345, and Ile2356, and thus poorly tolerant of a formal charge. Modifications of the ethyl urea were much less well tolerated; replacement of the nitrogen adjacent to the phenyl ring with an oxygen (**12f**) resulted in a 200-fold reduction in mTOR binding and an almost complete loss of selectivity against PI3Kα/δ. The second urea nitrogen was also replaced with oxygen (**12g**), resulting in a 20-fold reduction in binding, but no significant loss in selectivity. The requirement for hydrogen bond donors in both positions is consistent with our binding model, in which each of the urea nitrogens forms a hydrogen bond to the side chain of Asp2195.<sup>9</sup>

Having now developed a number of compounds potent in the biochemical assay, we examined their cellular activity in two separate assays. For this, we used the pTEN-null prostate carcinoma NCI-PC3 cell line, in which the loss of pTEN leads to phosphorylation of Akt at Thr308, activating the Akt kinase, which then phosphorylates and activates mTOR along with its other substrates. In this cell line, we measured the inhibition of the phosphorylation of Ser473 of Akt, a known mTORC2 substrate, and also assessed the antiproliferative activity of our

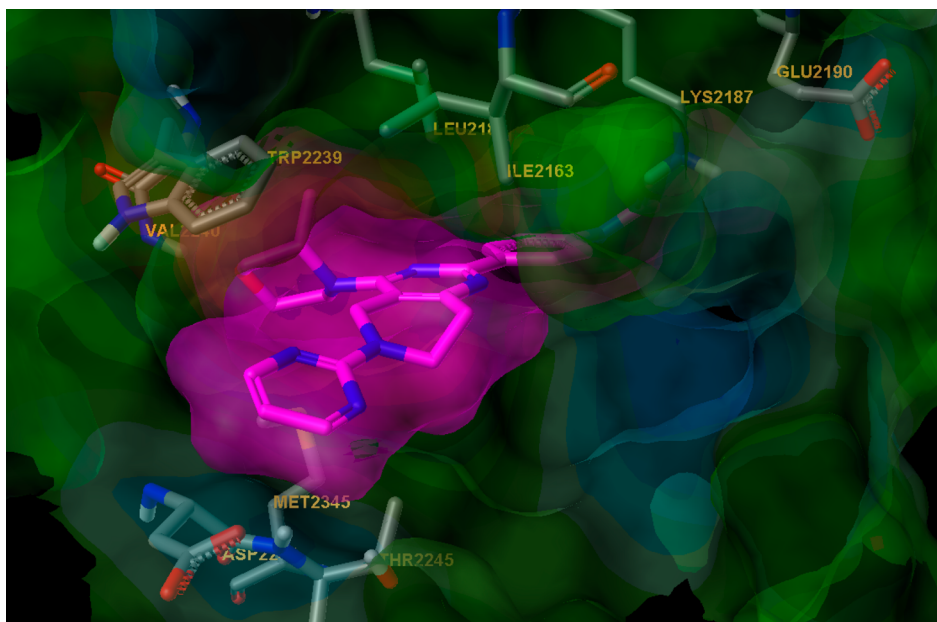
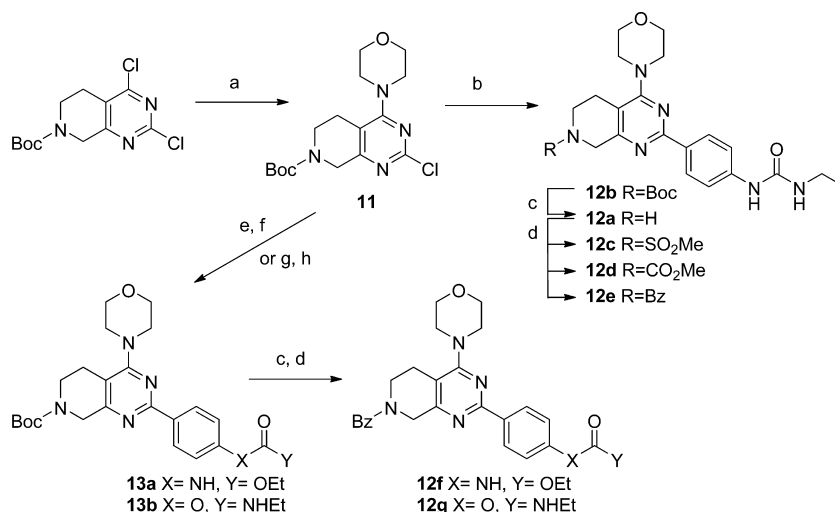


**Figure 2.** Compound **10f** docked into a homology model of mTOR that was built using PI3K $\gamma$  as a template.<sup>9</sup> Residues differing from those in PI3K $\gamma$  are labeled. The molecular surfaces for both ligand and protein are shown to illustrate the intimate interaction provided by the presence of the (*S*)-methyl substituent on the morpholine. The protein surface is color coded by hydrophobicity (tan-brown is hydrophobic, cyan-blue is hydrophilic, and green is in between). The ligand surface is magenta.

### Scheme 3. Synthesis of 7-Aza-tetrahydroquinazolines **12a–g**<sup>a</sup>

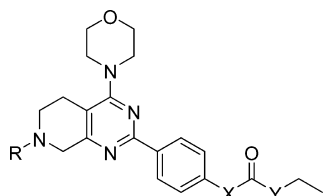


<sup>a</sup>Reagents and conditions: (a) morpholine, DIPEA; (b) (4-ethylurido)phenylboronic acid pinacol ester, Pd(PPh<sub>3</sub>)<sub>4</sub>, KOAc, Na<sub>2</sub>CO<sub>3</sub>, H<sub>2</sub>O/CH<sub>3</sub>CN, 120 °C; (c) TFA, CH<sub>2</sub>Cl<sub>2</sub>, then PS-carbonate resin; (d) electrophile, DIPEA, CH<sub>2</sub>Cl<sub>2</sub>; (e) 4-hydroxyphenylboronic acid pinacol ester, Pd(PPh<sub>3</sub>)<sub>4</sub>, KOAc, Na<sub>2</sub>CO<sub>3</sub>, H<sub>2</sub>O/CH<sub>3</sub>CN, 120 °C, 89%; (f) EtNCO, THF, 70 °C, 24 h, 38%; (g) 4-aminophenylboronic acid pinacol ester, Pd(PPh<sub>3</sub>)<sub>4</sub>, KOAc, Na<sub>2</sub>CO<sub>3</sub>, H<sub>2</sub>O/CH<sub>3</sub>CN, 120 °C, 86%; (h) ethyl chloroformate, THF, DIPEA, 70%.

compounds more broadly through determination of an IC<sub>50</sub> in a 3-day viability assay (Table 3). In each case, we found that cellular potency tracked roughly with the biochemical potency of the compounds, with compound **12h** being the most potent in both assays.

As it had been successful in the case of the 6-aza-tetrahydroquinazolines, we again attempted to improve the *in vitro* potency and selectivity of the 7-aza-tetrahydroquinazolin compounds by incorporating (*S*)-2-methylmorpholine as our hinge binder (Table 4). This proved successful, and we sought to better quantify the effect by evaluating the potency and selectivity of all 51 pairs of 7-aza-tetrahydroquinazolines in our

database. Each pair contained the phenethyl urea and differed only in the presence or absence of the 2-*S*-methyl group on the morpholine. Matched pair analysis<sup>33</sup> showed that the change in mTOR K<sub>i</sub> was modest over these pairs, with those molecules containing the methyl group being 3.2-fold more potent on average. The effect on selectivity was much more pronounced, with the methyl group containing compounds producing an average increase of 19.5-fold in selectivity for PI3K $\alpha$ . This is consistent with our modeling results, which predict an improved interaction with Trp2239 in mTOR as well as an unfavorable interaction with the larger phenylalanine residue in place of Leu2185 in PI3K $\alpha$ . We were unable to observe any

Table 3. In Vitro Data for 7-Aza-tetrahydroquinazoline Compounds 12a–h<sup>a</sup>


	R <sub>1</sub>	X	Y	mTOR K <sub>i</sub> (nM)	PI3K $\alpha/\delta$ (fold)	IC <sub>50</sub> (nM)	
						pAKT	MCI-PC3
12a	H	NH	NH	140	36/17	nd	nd
12b	Boc	NH	NH	12	48/79	22	nd
12c	MeSO <sub>2</sub>	NH	NH	21	10/50	43	430
12d	CO <sub>2</sub> Me	NH	NH	12	22/92	37	220
12e	Bz	NH	NH	6.5	38/86	22	340
12f	Bz	O	NH	1500	6.5/6.5	nd	nd
12g	Bz	NH	O	130	79/79	115	4800
12h	2-pyrimidine	NH	NH	5.5	60/130	25	290

<sup>a</sup>Assays are described in ref 30; nd = not determined.

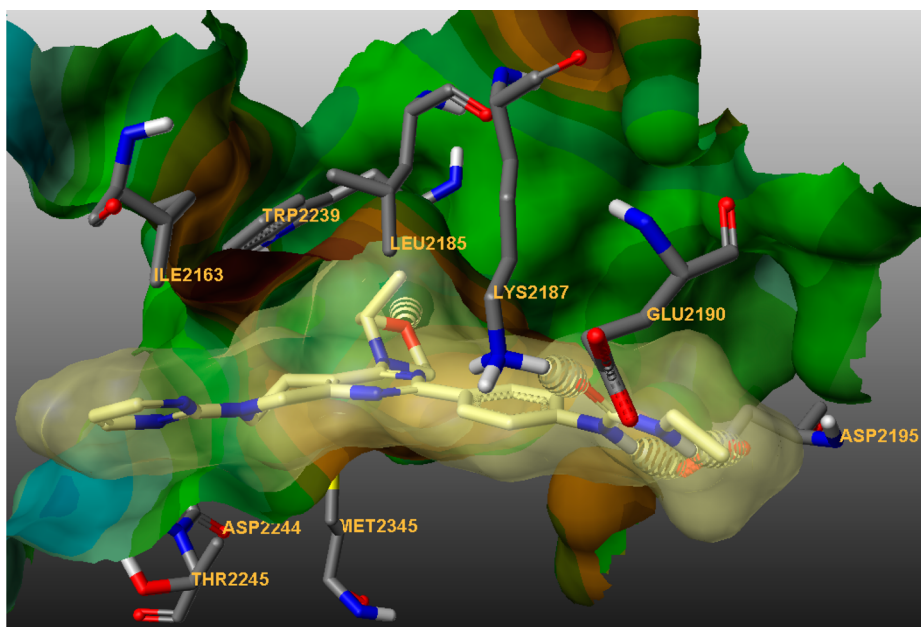


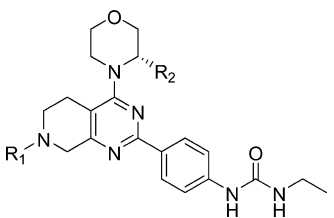
**Figure 3.** Compound 12i docked into a homology model of mTOR that was built using PI3K $\gamma$  as a template.<sup>9</sup> Residues differing from those in PI3K $\gamma$  are labeled. Predicted hydrogen-bonding interactions with the protein are shown as dashed ovals, and the molecular surfaces for both ligand and protein are shown to illustrate the intimate interaction provided by the presence of the (*S*)-methyl substituent on the morpholine. The protein surface is color coded by hydrophobicity (tan-brown is hydrophobic, cyan-blue is hydrophilic, and green is in between). The ligand surface is yellow.

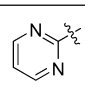
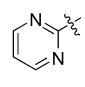
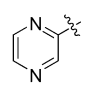
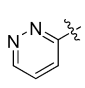
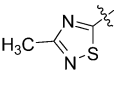
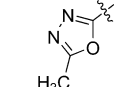
additional improvement in potency and or selectivity by incorporating a 2-*S*-ethylmorpholine in compound 12j.

Having determined that the 7-aza-tetrahydroquinazolines with a 2-*S*-methylmorpholine as hinge binding element provided superior potency and selectivity, we varied the heterocycles appended to the 7-position of our scaffold. We examined the diazines and a few additional electron-poor heterocycles, as shown in Table 4, and found that they exhibited similar single-digit nanomolar potency with selectivity varying, but almost always exceeding 100-fold against both PI3K $\alpha$  and PI3K $\delta$ . We observed the expected suppression of both mTORC1 and mTORC2 in a pTEN-null prostate carcinoma NCI-PC3 cell line<sup>34</sup> as measured by phosphorylation of p70S6K and Akt, respectively. We were pleased to observe potent antiproliferative activity for these compounds on both

the PTEN null NCI-PC3 prostate cell line as well as the MCF-7neo/Her2 breast cancer cell line, which has an activating mutation in PI3K. Additionally, compounds 12h–n showed no inhibition of the cytochrome P450 (CYP) mediated metabolism of standard substrates for the 3A4 (midazolam and testosterone), 2D6 (dextromethorphan), 2C9 (warfarin), 1A2 (phenacetin), or 2C19 (mephenytoin) isoforms,<sup>35</sup> indicating that they were at a reduced risk for drug–drug interactions when codosed with compounds metabolized principally by only one of these isoforms.

As compounds 12h–n exhibited similar potency and selectivity in our enzymatic assays as well as potent antiproliferative activity in two separate cell lines, we used a series of mouse PK studies to determine which were most suitable for advancement to in vivo tumor models. We included

Table 4. In Vitro Data for 7-Aza-tetrahydroquinazoline Compounds 12i–n<sup>a</sup>


	R1	R2	potency/selectivity		target modulation		proliferation	
			mTOR K <sub>i</sub> (nM)	PI3K α/δ (fold)	pAKT IC <sub>50</sub> (nM)	pp70S6K IC <sub>50</sub> (nM)	NCI-PC3 IC <sub>50</sub> (nM)	MCF7neo/Her2 IC <sub>50</sub> (nM)
12i		Me	1.5	500/>1000	3.3	9.1	150	57
12j		Et	1.3	410/>1000	1.5	nd	40	38
12k		Me	1.7	320/470	4.3	7.8	55	110
12l		Me	1.4	94/180	13	35	140	290
12m		Me	3.5	410/360	8.7	19	230	69
12n		Me	4.4	340/570	22	62	310	130

<sup>a</sup>Assays are described in ref 30; nd = not determined.

Table 5. In Vitro and in Vivo PK Data for Selected 7-Aza-tetrahydroquinazolines

	microsomal Cl <sub>hep</sub> <sup>b</sup> [(mL/min)/kg] h/r/m <sup>c</sup>	PPB (%) h/r/m <sup>c</sup>	mouse PK <sup>a</sup>					
			iv (1 mg/kg)			po (5 mg/kg)		
			Cl [(mL/min)/kg]	V <sub>ss</sub> (L/kg)	t <sub>1/2</sub> (h)	AUC (μm·h)	F%	
10f	16/44/71	98/97/97	38	2.4	1.7	2.9	62	
10h	15/44/80	97/96/97	120	1.4	0.18	0.41	29	
12h	13/31/40	98/99/99	22	1.1	0.7	5.7	70	
12i	15/33/61	98/97/99	36	1.2	1.7	2.0	42	
12l	7.3/19/34	nd <sup>d</sup>	44	1.7	0.75	0.87	21.8	
12m	19/29/58	97/96/98	22	0.72	0.53	2.5	32	

<sup>a</sup>Compound dosed iv as a solution in 80% PEG/10% EtOH and dosed po as a suspension in MCT. <sup>b</sup>Cl<sub>hep</sub> predicted from incubation with microsomes. <sup>c</sup>h/r/m = human/rat/mouse. <sup>d</sup>nd = not determined

similar compounds **10f** and **10h** from our 6-aza-tetrahydroquinazoline series for comparison as well. We were gratified to observe that a microsomal model of metabolic stability enabled us to predict the in vivo clearance of compounds **12** in mice fairly well (Table 5). The intravenous clearance for these compounds ranged from 24 to 49% of mouse liver blood flow while the bioavailability of these compounds ranged from 22 to 70%. Compound **12h** appeared most attractive overall, combining the lowest clearance with the highest oral bioavailability, resulting in an AUC after oral dosing which was 2-fold higher than that of the other 7-aza-tetrahydroquinazolines examined.

In addition to PK analysis, compound **12h** was examined in a panel of 250 kinases at a concentration of 1 μM. It proved

exquisitely selective with no inhibition greater than 25% observed in kinases other than mTOR and the three class I PI3Kα, -γ, and -δ, which were approximately 50% inhibited at 1 μM. Compounds **10f** and **12i** were spot checked against a smaller panel of 50 kinases and exhibited still greater selectivity, with no inhibition greater than 25% for any kinase assayed at 1 μM, including the PI3K isoforms. This illustrates the general nature of the selectivity derived from this scaffold and the still greater selectivity possible with 2-S-methylmorpholine used as the hinge binder.

At this point, we had a number of potent and selective compounds in hand that exhibited sufficiently long half-lives in vivo suitable for further study of the effects suppression of mTOR kinase activity has on antiproliferative potency. We

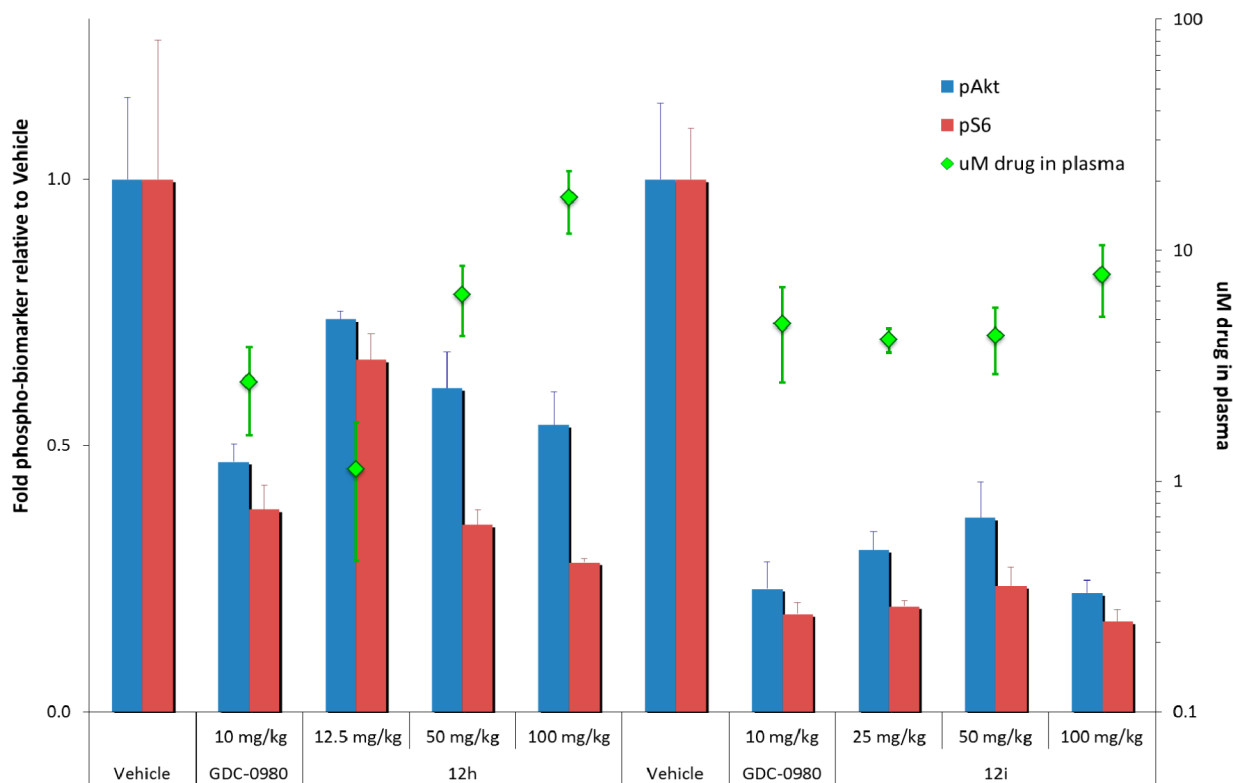


**Figure 4.** Plasma levels of 12h and 12i 6 h following oral administration in PC3 tumor-bearing mice along with the fold decreases of phosphorylated mTORC1 and -2 substrates relative to time-matched vehicle controls. Error bars represent one standard deviation from the depicted mean value. Four mice were dosed for each compound, and phosphoprotein levels were measured in duplicate samples for each mouse.

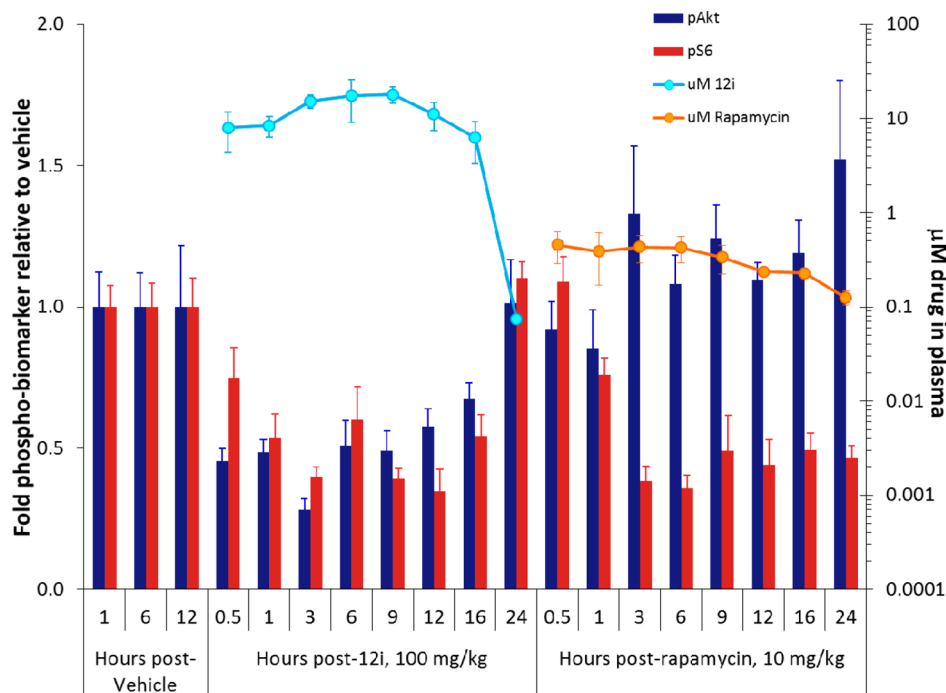


**Figure 5.** Plasma levels of 12i and rapamycin following administration in U87 tumor-bearing mice along with the fraction of phosphorylated mTORC1 and -2 substrates relative to time-matched vehicle controls. Error bars represent one standard deviation from the depicted mean value. Four mice were dosed for each compound and time point, and phosphoprotein levels were measured in duplicate samples for each mouse.

began by investigating the ability of these compounds to suppress signaling through the PI3K/Akt/mTOR pathway using NCI-PC3 prostate tumors implanted subcutaneously into Taconic NCR nude mice. Compounds 12h and 12i were

selected for this study due to their potency, selectivity, and favorable mouse PK profile.

After administration at three separate doses, tumor and plasma samples were obtained after 6 h (Figure 4). The plasma

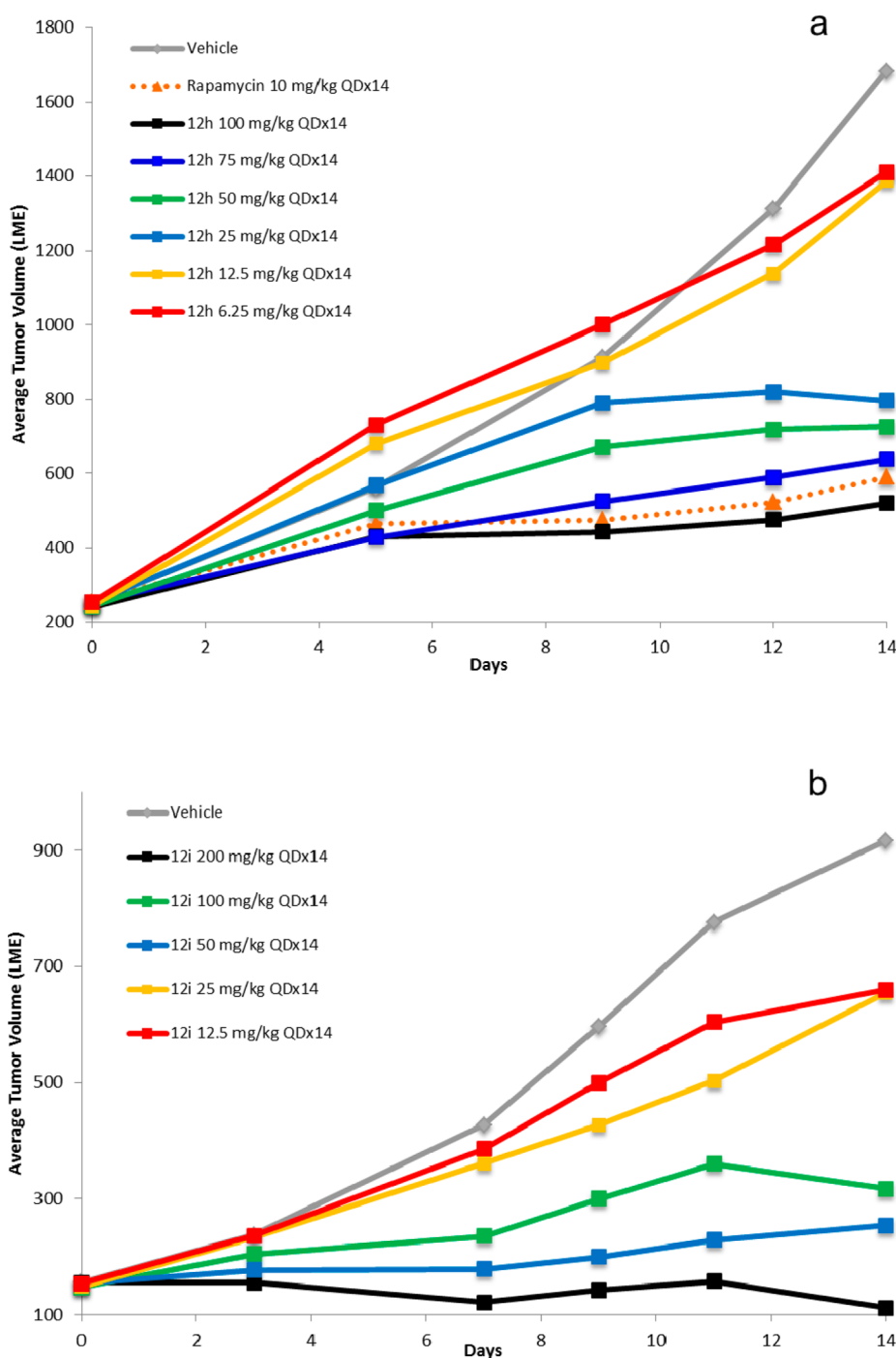


**Figure 6.** Growth inhibition curves for compounds **12h** (a) and **12i** (b) used to treat subcutaneously implanted PC3 tumors in mice.

levels observed for the two compounds were as expected on the basis of our previous oral administration in mice. The pharmacodynamic (PD) effect of our inhibitors was assessed by measuring the fold reduction of phospho-Ser437, normalized to total Akt, as well as the fold reduction of phospho-Ser235 and -236, normalized to total S6, relative to their time-matched vehicle control. Inhibition of S6 phosphorylation is indicative of inhibition of the mTORC1 complex, while inhibition of Akt phosphorylation is indicative of inhibition of the mTORC2 complex. Both molecules potently inhibited phosphorylation of both substrates after 6 h. The performance of each drug was comparable to that of 10 mg/kg GDC-0980, which was run as a contemporaneous positive

control and can be considered a benchmark of maximum knockdown for this model and assay method.<sup>36</sup> **12h** showed a dose response between 12.5 and 100 mg/kg, while all doses of **12i** tested performed similarly to GDC-0980. We did not repeat the study of **12i** at lower doses to determine the lowest dose capable of achieving full knockdown of mTOR substrates.

We next sought to evaluate the difference in inhibition profile between the present mTOR kinase inhibitors and rapamycin, which would be expected to reduce only phosphorylation of mTORC1 substrates such as S6. We therefore repeated our PK/PD experiment, sampling the tumor and blood over a 24 h period, comparing a 100 mg/kg dose of **12i** to a 10 mg/kg dose of rapamycin (Figure 5). In this instance, we used the U87



glioma model, which is also PTEN-deficient. By extending sampling to 24 h, we were able to observe the clearance of **12i** and the recovery of phospho-Akt and phospho-S6 levels to vehicle levels by the end of the experiment. As anticipated, we found that administration of rapamycin inhibited phosphorylation of S6, but did not reduce phospho-Akt levels. Instead, we observed the previously noted hyperphosphorylation of Akt on serine 473 at all time points beyond 1 h.

Having obtained an understanding of the extent of PI3K/Akt/mTOR pathway inhibition we could obtain from our compounds at a given dose and time point, we decided to probe the extent to which these compounds could suppress tumor growth in vivo. A 14-day efficacy study was run in the NCI-PC3 model, with daily dosing. **12h** was administered at doses from 6.25 to 100 mg/kg QD in an effort to span the range of pathway suppression observed in our PK/PD experiments. Rapamycin was dosed at 10 mg/kg, a dose previously determined to be efficacious in this model.

After 14 days of dosing, all animals remained on study, but the 100 mg/kg dose group had lost slightly more than 10% of their starting body weight, which triggers a dosing holiday in our protocol and indicates that we are approaching the maximum tolerated dose (MTD). By way of comparison, the vehicle group lost 3.7% of their body weight, as this model is mildly cachexic. The tumor growth curves (Figure 6a) were calculated by linear mixed effects (LME) modeling, and clearly illustrate that stronger pathway inhibition results in steadily increasing inhibition of growth and that tumor stasis has not been reached at the highest dose examined. The 10 mg/kg QD  $\times$  14 course of rapamycin performed well in this model, approaching tumor stasis. While tolerated, this dose achieves a greater rapamycin exposure level in mice than can be analogously achieved in humans,<sup>37–39</sup> which may account for its efficacy in this model.

We subsequently examined the growth inhibitory properties of the more potent **12i** in the same model, again at a range of doses. At the highest dose of 200 mg/kg dosed QD, we again observed body weight loss exceeding 10% at the end of the study. We observed stronger tumor growth inhibition at all doses of **12i** than was observed for **12h** at the identical dose. We again noted that maximum inhibition of tumor growth was only achieved at doses greater than that which could be tolerated by the mice without a dosing holiday over the course of a 2 week study (Figure 6b). In this study, we noted that the 50 mg/kg dose appeared more efficacious than the 100 mg/kg dose, but we attribute this to experimental variability resulting from our small cohort size of five animals per group. This was substantiated by the results of a second study performed simultaneously with material from the same lot of **12i**, in which we examined the effect of BID dosing at the same total dose per day. In this study, the 50 mg/kg/day dose resulted in slightly lower efficacy than the 100 mg/kg/day dose as measured by the average tumor volume (data not shown).

These studies clearly demonstrated that we had met our goal of producing a potent, selective, orally available inhibitor of the mTOR kinase. Our compounds robustly inhibited tumor growth in cell lines in which the PI3K/Akt/mTOR signaling pathway is constitutively active due to the loss of PTEN. **12i** achieved tumor stasis at the highest 200 mg/kg/day dose examined, which appears to also be approaching the limit of tolerability for this molecule.

## CONCLUSIONS

We have developed a novel class of potent, highly selective mTOR kinase domain antagonists. The addition of saturated heterocycles fused to the central pyrimidine ring, along with the previously described phenyl ethyl urea and *S*-methylmorpholine hinge binder provided compounds with nanomolar in vitro potency and high selectivity against PI3K and other kinases.

This biochemical potency translated into potent growth inhibition in cell lines where the PI3K/Akt/mTOR signaling pathway is constitutively active due to the loss of PTEN or due to an activating mutation in PI3K. Compounds **12h** and **12i** suppressed mTORC1 and mTORC2 in cellular and in vivo PK/PD experiments and did not induce the hyperphosphorylation of Akt as rapamycin did at time points after 3 h. This potential advantage did not, however, translate into greater efficacy in our PC3 xenograft model when rapamycin and mTOR inhibitors were compared at doses approaching their MTD in mice. This may be due in part to the fact that the rapamycin levels achieved in mice cannot be reproduced in man, limiting its efficacy. What remains to be understood is whether the tolerability in man of these different modes of pathway inhibition differs and whether mTOR can be effectively combined with other targeted chemotherapeutics. Compounds **12h** and **12i** were found to exhibit time-dependent inhibition of CYP 3A4, which prevented their progression into the clinic; however, further refinement of this scaffold enabled us to select a clinical candidate that joined the PI3K selective and dual PI3K/mTOR inhibitors undergoing human clinical trials in an effort to address these questions directly.

## EXPERIMENTAL SECTION

All chemicals were purchased from commercial suppliers and used as received. Flash chromatography was carried out with prepacked silica cartridges from either ISCO or SiliCycle on an ISCO Companion chromatography system using gradient elution. NMR spectra were recorded on a Bruker AV III 400 or 500 NMR spectrometer and referenced to tetramethylsilane. Preparative HPLC was performed on a Polaris C18 5  $\mu$ m column (50 mm  $\times$  21 mm), eluting with mixtures of water/acetonitrile. All final compounds were purified to >95% chemical and optical purity, as assayed by LC/MS. This analysis was performed on an Agilent 1100 HPLC coupled with Agilent MSD mass spectrometer using ESI as the ionization source. The LC separation was performed using an Agilent ZORBAX SB-C18, 1.8 mm, 30  $\times$  2.1 mm column with a flow rate of 0.4 mL/min. The gradient consisted of 3–97% acetonitrile in water, each containing 0.05% TFA, over 7 min; 97% acetonitrile was then maintained for 1.5 min, followed by reequilibration at 3% acetonitrile for 1.5 min. The LC column temperature was maintained at 40 °C. UV absorbance was measured at 220 and 254 nm along with a full scan mass spectrum. For select compounds, a longer gradient LC was used (method B). In these cases, the gradient consisted of 2–98% acetonitrile in water, each containing 0.05% TFA, over 25.5 min; 98% acetonitrile was then maintained for 2.5 min, followed by reequilibration at 2% acetonitrile for 1.5 min. UV and MS detection was performed as before.

**In-Life PK–PD Study.** Human prostate cancer NCI-PC3 cells (National Cancer Institute, Frederick, MD) were implanted subcutaneously into the right hind flanks of female NCR nude mice (5  $\times$  10<sup>6</sup> cells in 100  $\mu$ L of Hank's balanced salt solution). Tumors were monitored until they reached a mean tumor volume of approximately 500 mm<sup>3</sup>. Then similarly sized tumors were randomly assigned to groups ( $n = 4$ ). Compounds were formulated as suspensions in 0.5% methylcellulose/0.2% Tween 80 (MCT) and dosed orally at 25, 50, and 100 mg/kg (100  $\mu$ L dose/25 g animal). Tumor and plasma samples were harvested at 1, 6, and 10 h postdose.

Blood samples were harvested by terminal cardiac puncture and collected into tubes containing K<sub>2</sub>EDTA as an anticoagulant. Samples

were kept chilled on ice until centrifugation at (1500–2000)g for 5 min; plasma was transferred to a new vial and snap frozen. Tumor samples were transferred to a 1.5 mL snap-cap polypropylene tube, weighed, and then flash frozen on dry ice. Samples were stored at –80 °C prior to PD biomarker evaluation.

**Xenograft Tumor Lysates.** Frozen tumors were lysed in ice-cold extraction buffer by mechanical disruption and agitation with a garnet/ceramic sphere matrix in a FastPrep-24 (MP Biomedicals, Solon, OH; five 20-s cycles with rest periods on wet ice). Extraction buffer (Biosource, Carlsbad, CA) was supplemented with protease inhibitors (F. Hoffman-La Roche, Mannheim, Germany), 1 mM phenylmethanesulfonyl fluoride, and phosphatase inhibitor cocktails 1 and 2 (Sigma-Aldrich, St. Louis, MO). After thorough disruption, tumor lysates were clarified by centrifugation at 4 °C. Protein concentrations were determined using the BCA protein assay kit (Pierce, Rockford, IL) and normalized to a standard concentration of 5 mg/mL.

**PD Biomarker Assays.** The Meso Scale Discovery Multi-Spot biomarker detection system (Meso Scale Discovery, Gaithersburg, MD) was used to determine the levels of Akt phosphorylated at Ser473 (pAkt) and S6RP phosphorylated at Ser235/236 (pS6RP). These double-determinant immunoassays quantify protein levels on the basis of measurements of electrochemoluminescence intensity. In the case of pS473 and total Akt, both of these were measured in the same well using a duplex assay plate. All other markers required separate plates to measure phosphorylated and total protein. Protein was loaded at 20 µg/well for Akt and 10 µg/well for S6RP.

Relative levels of phosphoprotein were determined by comparison of treated tumor lysates with an average of the time-matched vehicle controls.

**In-Life Efficacy Study.** NCI-PC3 cells were subcutaneously implanted as above. Tumors were grown to an average volume of 200 mm<sup>3</sup> before dosing was started. Extra mice were implanted, to ensure that each treatment group of 5 mice had similarly sized tumors. Tumor volumes were determined using digital calipers (Fred V. Fowler Co., Inc.) using the formula  $(L \times W \times H)/2$ . Average tumor volume was calculated by applying curve fitting to the log 2 transformed individual tumor volume data using a linear mixed-effects model using the R package nlme, version 3.1–97 in R v2.12.0. Percent tumor growth inhibition, %TGI, was calculated as the percentage of the area under the fitted curve (AUC) for the respective dose group per day in relation to the vehicle, such that  $\%TGI = 100 \times 1 - (AUC_{\text{treatment/day}}/AUC_{\text{vehicle/day}})$ . Tumors were measured and mice weighed twice per week. If weight loss was >15%, the mice were weighed daily and euthanized if weight loss reached 20%; 10% body weight loss was the limit for tolerated doses. Mice whose tumors reached 2000 mm<sup>3</sup> were euthanized.

**tert-Butyl 2-Chloro-4-morpholino-5H-pyrrolo[3,4-d]pyrimidine-6(7H)-carboxylate.** To a mixture of *tert*-butyl 2,4-dichloro-5H-pyrrolo[3,4-d]pyrimidine-6(7H)-carboxylate (1.2 g, 4.1 mmol) and *N,N*-diisopropylamine (1.4 mL, 8.3 mmol) in 2-propanol (8 mL) was added morpholine (0.430 mL, 5.0 mmol). The mixture was stirred at room temperature for 1 h and was then concentrated in vacuo. The resulting residue was purified by flash column chromatography (40% EA/Hex) to give *tert*-butyl 2-chloro-4-morpholino-5H-pyrrolo[3,4-d]pyrimidine-6(7H)-carboxylate (1.378 g, 98%).

**tert-Butyl 2-(4-(3-Ethylureido)phenyl)-4-morpholino-5H-pyrrolo[3,4-d]pyrimidine-6(7H)-carboxylate (6a).** 2-Chloro-4-morpholino-5H-pyrrolo[3,4-d]pyrimidine-6(7H)-carboxylate (0.366 mmol), (4-ethylureido)phenylboronic acid pinacol ester (0.439 mmol), tetrakis(triphenylphosphine)palladium (0.022 mmol), 1 M aq KOAc (0.55 mL), 1 M aq Na<sub>2</sub>CO<sub>3</sub> (0.55 mL), and MeCN (2 mL) were mixed in a microwave reaction tube. The mixture was heated in a microwave reactor at 120 °C for 25 min. The mixture was extracted with EtOAc (3×), and the combined organic extracts were concentrated. The resulting residue was purified by flash column chromatography (40% EA/Hex) to give **6a** (149 mg, 83%). LC/MS: 4.43 min, M<sup>+</sup> = 469.2, MW = 468.6. <sup>1</sup>H NMR (500 MHz, CDCl<sub>3</sub>): δ 8.28 (d, J = 8.7, 2H), 7.38 (d, J = 8.8, 2H), 7.10 (d, J = 8.6, 1H), 6.81

(d, J = 8.8, 1H), 4.78 (s, 2H), 4.57 (s, 2H), 3.93–3.59 (m, 8H), 3.36–3.29 (m, 2H), 1.53 (s, 9H), 1.17 (t, J = 7.2, 3H).

**1-Ethyl-3-(4-(4-morpholino-6,7-dihydro-5H-pyrrolo[3,4-d]pyrimidin-2-yl)phenyl)urea (6b).** *tert*-Butyl 2-(4-(3-ethylureido)phenyl)-4-morpholino-5H-pyrrolo[3,4-d]pyrimidine-6(7H)-carboxylate (1.74 mmol) was dissolved in CH<sub>2</sub>Cl<sub>2</sub> (5 mL), and then TFA (3 mL) was added. The mixture was stirred at room temperature for 2 h. 2-Propanol and toluene were added, and the resulting mixture was concentrated in vacuo. The resulting residue was azeotroped with toluene two more times. Methanol and methylene chloride (4 mL of each) were added to the resulting residue, then PS-carbonate (2.5–3.5 mmol N/g resin, 1.45 g) was added. The mixture was stirred at room temperature until the pH reached >7 (~1 h). The mixture was filtered, and the resin was washed with methanol and CH<sub>2</sub>Cl<sub>2</sub>. The filtrate was concentrated to provide **6b**, which was used without further purification in subsequent reactions. A portion of the material was purified by reverse-phase HPLC for assay. LC/MS: 2.74 min, M<sup>+</sup> = 369.2, MW = 368.4. <sup>1</sup>H NMR (400 MHz, DMSO-*d*<sub>6</sub>): δ 9.57 (s, 1H), 8.75 (s, 1H), 8.19 (d, J = 8.9, 2H), 7.50 (d, J = 8.9, 2H), 6.38–6.08 (m, 1H), 4.71 (s, 2H), 4.38 (s, 2H), 3.72 (s, 8H), 3.24–3.03 (m, 2H), 1.06 (t, J = 7.2, 3H).

**1-Ethyl-3-(4-(4-morpholino-6-(pyrimidin-2-yl)-6,7-dihydro-5H-pyrrolo[3,4-d]pyrimidin-2-yl)phenyl)urea (6c).** **6b** (0.15 mmol), 2-chloropyrimidine (0.21 mmol), and *i*-PrN<sub>2</sub>Et (0.6 mmol) were mixed in DMF (0.6 mL) in a microwave reaction tube. The mixture was heated to 120 °C and stirred for 15 min. After cooling to room temperature, the mixture was diluted with DMF. The resulting mixture was purified by reverse-phase HPLC to give **6c**. LC/MS: 3.80 min, M<sup>+</sup> = 447.3, MW = 446.5. <sup>1</sup>H NMR (500 MHz, DMSO-*d*<sub>6</sub>): δ 8.71 (s, 1H), 8.47 (d, J = 4.8, 2H), 8.21 (d, J = 8.8, 2H), 7.51 (d, J = 8.8, 2H), 6.77 (t, J = 2.5, 1H), 6.18 (m, 1H), 4.99 (s, 2H), 4.68 (s, 2H), 3.78 (m, 8H), 3.20–3.15 (m, 2H), 1.26 (t, J = 6.9, 3H). LC/MS: *m/z* = +447 (M + H)<sup>+</sup>.

**1-Ethyl-3-(4-(6-(methylsulfonyl)-4-morpholino-6,7-dihydro-5H-pyrrolo[3,4-d]pyrimidin-2-yl)phenyl)urea (6d).** LC/MS: 3.59 min, M<sup>+</sup> = 447.2, MW = 446.5. <sup>1</sup>H NMR (400 MHz, DMSO-*d*<sub>6</sub>): δ 8.69 (s, 1H), 8.18 (d, J = 8.7, 2H), 7.49 (d, J = 8.8, 2H), 6.19 (br s, 1H), 4.84 (s, 2H), 4.51 (s, 2H), 4.04–3.76 (m, 8H), 3.20–3.08 (m, 2H), 3.06 (s, 3H), 1.06 (t, J = 7.2, 3H).

**Ethyl 2-(4-(3-Ethylureido)phenyl)-4-morpholino-5H-pyrrolo[3,4-d]pyrimidine-6(7H)-carboxylate (6e).** LC/MS: 3.53 min, M<sup>+</sup> = 440.3, MW = 439.5. <sup>1</sup>H NMR (500 MHz, DMSO-*d*<sub>6</sub>): δ 8.73 (s, 1H), 8.18 (d, J = 6.7, 2H), 7.49 (d, J = 8.8, 2H), 6.26–6.15 (m, 1H), 4.82 (d, J = 13.9, 2H), 4.50 (d, J = 15.2, 2H), 4.21–4.07 (m, 2H), 3.80–3.69 (m, 8H), 3.19–3.06 (m, 2H), 1.25 (t, J = 7.0, 3H), 1.06 (t, J = 7.2, 3H).

**6-Benzyl-5,6,7,8-tetrahydropyrido[4,3-d]pyrimidine-2,4-(1H,3H)-dione.** Methyl 1-benzyl-4-oxo-3-piperidinecarboxylate (20.194 g, 71.168 mmol) and urea (9.031 g, 150.4 mmol) were dissolved in methanol (150 mL, 3700 mmol), and 46 mL of a 1 M solution of sodium methoxide in methanol was added dropwise. Then, the reaction was heated to reflux under N<sub>2</sub> for 96 h. The reaction was cooled to 0 °C and filtered to give a white solid. This was stirred vigorously for 30 min with 50 mL of water, cooled to 0 °C, and filtered to give 6-benzyl-5,6,7,8-tetrahydropyrido[4,3-d]pyrimidine-2,4-(1H,3H)-dione as a white solid (11.77 g, 45.7 mmol) which was dried under high vacuum overnight and then used without further purification. <sup>1</sup>H NMR (DMSO-*d*<sub>6</sub>, 400 MHz): δ 7.47–7.07 (m, 5H), 3.56 (s, 2H), 2.96 (s, 2H), 2.51 (t, 4H), 2.27 (t, J = 5.6, 2H).

**6-Benzyl-2,4-dichloro-5,6,7,8-tetrahydropyrido[4,3-d]pyrimidine (7).** 6-Benzyl-5,6,7,8-tetrahydropyrido[4,3-d]pyrimidine-2,4-(1H,3H)-dione (16.95 g, 65.88 mmol) was added to phosphoryl chloride (100 mL, 1070 mmol) in a 500 mL round-bottom flask equipped with a stirbar, and the solution was refluxed for 3 h under N<sub>2</sub>. The volatiles were removed under reduced pressure, and the concentrate was poured over 250 mL of ice. NaOH (3 M) was added to a final pH of 10, and then the aqueous phase was extracted with CH<sub>2</sub>Cl<sub>2</sub> (3 × 150 mL). The combined organics were dried over MgSO<sub>4</sub>, filtered, and concentrated to a tan oil. This crude material was dissolved in dichloromethane, concentrated onto silica gel, and

subjected to column chromatography using a 120 g column, with a gradient of 0%–50% ethyl acetate in hexanes. The product-containing fractions were combined and evaporated under reduced pressure to give **7** as a pale solid (14.63 g, 49.7 mmol). <sup>1</sup>H NMR (CDCl<sub>3</sub>, 400 MHz): δ 7.41–7.27 (m, 5H), 3.77 (s, 2H), 3.62 (s, 2H), 2.99 (t, J = 5.8, 2H), 2.81 (t, J = 5.8, 2H).

**tert-Butyl 2,4-Dichloro-7,8-dihydropyrido[4,3-d]pyrimidine-6(5H)-carboxylate (8).** Compound **7** (1.84 g, 6.25 mmol) was dissolved in methylene chloride (40 mL, 700 mmol) in a round-bottom flask equipped with a stirbar and the reaction was cooled to 0 °C. *α*-Chloroethyl chloroformate (0.810 mL, 7.50 mmol) was added slowly and the reaction was stirred at 0 °C for 15 min. The reaction was allowed to warm to room temperature (rt) and then was refluxed for 1 h. The volatiles were removed under reduced pressure, and the residue was redissolved in 20 mL of MeOH and heated to reflux for 30 min. The volatiles were removed under reduced pressure to give the intermediate amine hydrochloride salt. This material was dissolved in 50 mL of dry CH<sub>2</sub>Cl<sub>2</sub>, to which was added 3.1 g of tetraalkylammonium carbonate polymer-bound (2.5–3.5 mmol N/g) resin and di-*tert*-butyldicarbonate (2.45 g, 11.2 mmol). The mixture was stirred at rt for 1 h and was then filtered to remove the resin. The crude mixture was concentrated onto silica gel and subjected to column chromatography using a 12 g column, eluting with a gradient of 0–30% EtOAc in hexanes. The product-containing fractions were combined and evaporated under reduced pressure to give **8** as a clear oil which slowly crystallized (1.68 g, 5.52 mmol). <sup>1</sup>H NMR (CDCl<sub>3</sub>, 400 MHz): δ 4.56 (s, 2H), 3.75 (t, J = 5.9, 2H), 2.97 (t, J = 5.8, 2H), 1.50 (s, 9H).

**tert-Butyl 2-(4-(3-Ethylureido)phenyl)-4-morpholino-7,8-dihydropyrido[4,3-d]pyrimidine-6(5H)-carboxylate (10a).** LC/MS: 4.97 min, M<sup>+</sup> = 483.3, MW = 482.6. <sup>1</sup>H NMR (DMSO-*d*<sub>6</sub>, 400 MHz): δ 8.67 (s, 1H), 8.19 (d, J = 8.7, 2H), 7.48 (d, J = 8.8, 2H), 6.18 (t, J = 5.5, 1H), 4.42 (s, 2H), 3.78–3.70 (m, J = 4.6, 4H), 3.67 (t, J = 6.2, 2H), 3.44–3.36 (m, J = 4.5, 4H), 3.17–3.05 (m, 2H), 2.85 (t, J = 6.2, 2H), 1.41 (s, 9H), 1.06 (t, J = 7.2, 3H).

**(S)-tert-Butyl 2-(4-(3-Ethylureido)phenyl)-4-(3-methylmorpholino)-7,8-dihydropyrido[4,3-d]pyrimidine-6(5H)-carboxylate (10b).** LC/MS: 5.22 min, M<sup>+</sup> = 497.3, MW = 496.6. <sup>1</sup>H NMR (DMSO-*d*<sub>6</sub>, 400 MHz): δ 8.66 (s, 1H), 8.18 (d, J = 8.8, 2H), 7.48 (d, J = 8.8, 2H), 6.18 (s, 1H), 4.47 (d, J = 16.0, 1H), 4.38 (d, 1H), 3.88 (d, J = 11.4, 2H), 3.76–3.35 (m, 7H), 3.19–3.03 (m, 2H), 2.85 (t, J = 6.2, 2H), 1.41 (s, 9H), 1.25 (d, J = 6.2, 3H), 1.06 (t, J = 7.2, 3H).

**(S)-1-Ethyl-3-(4-(4-(3-methylmorpholino)-6-(methylsulfon-yl)-5,6,7,8-tetrahydropyrido[4,3-d]pyrimidin-2-yl)phenyl)urea (10c).** LC/MS: 2.51 min, M<sup>+</sup> = 475.2, MW = 474.6. <sup>1</sup>H NMR (500 MHz, DMSO-*d*<sub>6</sub>): δ 8.69 (s, 1H), 8.26–8.11 (m, 2H), 7.59–7.40 (m, 2H), 6.18 (t, J = 5.5 Hz, 1H), 4.34–4.12 (m, 2H), 4.01–3.80 (m, 2H), 3.72 (dd, J = 11.4, 2.9 Hz, 1H), 3.70–3.56 (m, 3H), 3.54–3.39 (m, 3H), 3.12 (dt, J = 12.7, 7.0 Hz, 2H), 3.03 (s, 3H), 2.99 (t, J = 6.4 Hz, 2H), 2.08 (s, 1H), 1.22 (d, J = 6.5 Hz, 3H), 1.06 (t, J = 7.2 Hz, 3H).

**(S)-1-(4-(6-Acetyl-4-(3-methylmorpholino)-5,6,7,8-tetrahydropyrido[4,3-d]pyrimidin-2-yl)phenyl)-3-ethylurea (10d).** LC/MS: 2.25 min, M<sup>+</sup> = 439.2, MW = 438.5. <sup>1</sup>H NMR (400 MHz, DMSO-*d*<sub>6</sub>): δ 8.66 (s, 1H), 8.24–8.12 (m, 2H), 7.53–7.42 (m, 2H), 6.17 (t, J = 5.7 Hz, 1H), 4.71–4.33 (m, 2H), 4.03–3.55 (m, 6H), 3.54–3.37 (m, 2H), 3.12 (qd, J = 7.2, 5.6 Hz, 2H), 2.95 (t, J = 5.9 Hz, 1H), 2.82 (t, J = 6.4 Hz, 1H), 2.15–2.02 (m, 3H), 1.32–1.19 (m, 3H), 1.06 (t, J = 7.2 Hz, 3H).

**1-Ethyl-3-(4-(4-morpholino-6-(pyrimidin-2-yl)-6,7-dihydro-5H-pyrrolo[3,4-d]pyrimidin-2-yl)phenyl)urea (10e).** 1-Ethyl-3-(4-(4-morpholino-6,7-dihydro-5H-pyrrolo[3,4-d]pyrimidin-2-yl)-phenyl)urea (0.15 mmol), 2-chloropyrimidine (0.21 mmol) and DIPEA (0.6 mmol) were mixed in DMF (0.6 mL) in a microwave reaction tube. The mixture was heated to 120 °C and stirred for 15 min. After cooling to room temperature, the mixture was diluted with DMF. The resulting mixture was purified by reverse-phase HPLC to give **9e**. LC/MS: 3.94 min, M<sup>+</sup> = 461.3, MW = 460.5. <sup>1</sup>H NMR (DMSO-*d*<sub>6</sub>, 400 MHz): δ 8.64 (s, 1H), 8.40 (d, J = 4.7, 2H), 8.18 (d, J = 8.7, 2H), 7.47 (d, J = 8.8, 2H), 6.66 (t, J = 4.7, 1H), 6.15 (t, J = 5.6, 1H), 4.85 (s, 2H), 4.10 (t, J = 6.2, 2H), 3.83–3.72 (m, 4H), 3.52–3.42

(m, 4H), 3.18–3.04 (m, 2H), 2.92 (t, J = 6.1, 2H), 1.06 (t, J = 7.2, 3H).

**(S)-1-Ethyl-3-(4-(4-(3-methylmorpholino)-6-(pyrimidin-2-yl)-5,6,7,8-tetrahydropyrido[4,3-d]pyrimidin-2-yl)phenyl)urea (10f).** LC/MS: 4.92 min, M<sup>+</sup> = 475.3, MW = 474.6. <sup>1</sup>H NMR (DMSO-*d*<sub>6</sub>, 400 MHz): δ 8.66 (s, 1H), 8.40 (d, J = 4.7, 2H), 8.17 (d, J = 8.7, 2H), 7.47 (d, J = 8.8, 2H), 6.65 (t, J = 4.7, 1H), 6.18 (t, J = 5.5, 1H), 4.93 (d, J = 16.1, 1H), 4.75 (d, J = 16.1, 1H), 4.25–4.12 (m, 1H), 4.06–3.95 (m, 2H), 3.90 (d, J = 11.3, 1H), 3.79–3.60 (m, 3H), 3.58–3.41 (m, 2H), 3.17–3.05 (m, 2H), 2.93 (t, J = 6.1, 2H), 1.27 (d, J = 6.6, 3H), 1.06 (t, J = 7.2, 3H).

**1-Ethyl-3-(4-(4-morpholino-6-(pyrazin-2-yl)-5,6,7,8-tetrahydropyrido[4,3-d]pyrimidin-2-yl)phenyl)urea (10g).** LC/MS: 3.83 min, M<sup>+</sup> = 461.3, MW = 460.5. <sup>1</sup>H NMR (DMSO-*d*<sub>6</sub>, 400 MHz): δ 8.64 (s, 1H), 8.42 (s, 1H), 8.18 (d, J = 8.7, 2H), 8.11 (s, 1H), 7.85 (d, J = 2.6, 1H), 7.47 (d, J = 8.7, 2H), 6.16 (t, J = 5.6, 1H), 4.70 (s, 2H), 3.98 (t, J = 6.2, 2H), 3.86–3.72 (m, 5H), 3.52–3.41 (m, 4H), 3.19–3.05 (m, 2H), 2.97 (t, J = 6.1, 2H), 1.06 (t, J = 7.2, 3H).

**(S)-1-Ethyl-3-(4-(4-(3-methylmorpholino)-6-(pyrazin-2-yl)-5,6,7,8-tetrahydropyrido[4,3-d]pyrimidin-2-yl)phenyl)urea (10h).** LC/MS: 4.72 min, M<sup>+</sup> = 475.3, MW = 474.6. <sup>1</sup>H NMR (DMSO-*d*<sub>6</sub>, 400 MHz): δ 8.65 (s, 1H), 8.41 (s, 1H), 8.17 (d, J = 8.7, 2H), 7.85 (d, J = 2.6, 1H), 7.47 (d, J = 8.8, 2H), 6.17 (t, J = 5.5, 1H), 4.76 (d, J = 16.1, 1H), 4.61 (d, J = 16.1, 1H), 4.08–3.98 (m, 2H), 3.96–3.84 (m, 3H), 3.78 (d, J = 8.6, 1H), 3.66 (t, J = 9.8, 3H), 3.56–3.42 (m, 3H), 3.17–3.05 (m, 2H), 2.97 (t, J = 6.1, 2H), 1.27 (d, J = 6.6, 4H), 1.06 (t, J = 7.2, 3H).

**tert-Butyl 2-Chloro-4-morpholino-5,6-dihydropyrido[3,4-d]pyrimidine-7(8H)-carboxylate (11).** To a solution of *tert*-butyl 2,4-dichloro-5,6-dihydropyrido-[3,4-*d*]pyrimidine-7(8H)-carboxylate (1.020 g, 3.353 mmol) in isopropyl alcohol (8.00 mL, 0.104 mol) was added *N,N*-diisopropylethylamine (1.15 mL, 0.0066 mol) followed by addition of morpholine (0.350 mL, 0.00401 mol) in a single portion. The resulting solution was stirred for 2 h at rt. The volatiles were removed under reduced pressure, and then the resulting white residue was partitioned between EtOAc (100 mL) and water (100 mL). The layers were separated, and the aqueous layer was washed with EtOAc (2 × 50 mL). The combined organic extracts were dried over MgSO<sub>4</sub>, filtered, and concentrated to a white solid. This crude material was dissolved in CH<sub>2</sub>Cl<sub>2</sub> and concentrated onto silica gel before being subjected to column chromatography using a 40 g column, with a gradient of 0% to 40% ethyl acetate in hexanes. The product-containing fractions were combined and evaporated under reduced pressure to give *tert*-butyl 2-chloro-4-morpholino-5,6-dihydropyrido[3,4-*d*]pyrimidine-7(8H)-carboxylate as a white solid (1.114 g, 3.14 mmol).

**tert-Butyl 2-(4-(3-Ethylureido)phenyl)-4-morpholino-5,6-dihydropyrido[3,4-d]pyrimidine-7(8H)-carboxylate (12b).** *tert*-Butyl 2-chloro-4-morpholino-5,6-dihydropyrido[3,4-*d*]pyrimidine-7(8H)-carboxylate (0.5784 g, 1.630 mmol), [4-(ethylureido)phenyl]-boronic acid, pinacol ester (0.5749 g, 1.981 mmol), and tetrakis-(triphenylphosphine)palladium(0) (205 mg, 0.177 mmol) were weighed into a microwave vial. Acetonitrile (6 mL, 100 mmol), degassed 1 M Na<sub>2</sub>CO<sub>3</sub> in water (2.2 mL), and degassed 1 M KOAc in water (2.2 mL) were added, and the mixture was heated to 120 °C for 15 min. The reaction was diluted with 50 mL of water and extracted with EtOAc (3 × 50 mL). Approximately ~10 mL of brine was added to aid in separating the layers. The combined organic extracts were dried with MgSO<sub>4</sub>, filtered, and concentrated onto silica gel. This crude material was then subjected to column chromatography using a 40 g column, with a gradient of 20%–50% ethyl acetate in CH<sub>2</sub>Cl<sub>2</sub>. The product-containing fractions were combined and evaporated under reduced pressure to give **12b** (0.785 g, 1.63 mmol). LC/MS: 4.53 min, M<sup>+</sup> = 483.3, MW = 482.6. <sup>1</sup>H NMR (DMSO-*d*<sub>6</sub>, 400 MHz): δ 8.63 (s, 1H), 8.18 (d, J = 8.7, 2H), 7.48 (d, J = 8.8, 2H), 6.14 (s, 1H), 4.46 (s, 2H), 3.90 (s, 1H), 3.73 (s, 4H), 3.49 (d, J = 22.0, 6H), 3.18–3.06 (m, 2H), 2.66 (s, 2H), 1.46 (s, 9H), 1.09–1.03 (m, 8H).

**1-Ethyl-3-(4-(4-morpholino-5,6,7,8-tetrahydropyrido[3,4-d]pyrimidin-2-yl)phenyl)urea (12a).** To **12b** (0.568 g, 1.00 mmol) in a 100 mL round-bottom flask equipped with a stirbar was added TFA (3.0 mL, 39 mmol) in a single portion. The reaction was stirred at rt

for 1 h. The volatiles were removed under reduced pressure, and the resulting oil was washed with Et<sub>2</sub>O, which produced a white solid precipitate. The precipitate was filtered off, dissolved in CH<sub>2</sub>Cl<sub>2</sub> and MeOH, and stirred with 1.0 g of PS-carbonate resin (2.5–3.6 mmol N/g) for 1 h at rt. The resin was filtered off and washed with CH<sub>2</sub>Cl<sub>2</sub>. The filtrate was then concentrated to give **12a** as a white solid (0.326 g, 8.52 mmol), which was used without further purification in subsequent reactions. A portion of the material was purified by reverse-phase HPLC for assay. LC/MS: 2.99 min, M<sup>+</sup> = 383.3, MW = 382.5. <sup>1</sup>H NMR (DMSO-*d*<sub>6</sub>, 400 MHz): δ 8.66 (s, 1H), 8.18 (d, J = 8.8, 2H), 7.47 (d, J = 8.8, 2H), 6.17 (t, J = 5.6, 1H), 3.86 (s, 2H), 3.77–3.70 (m, 4H), 3.47–3.40 (m, 4H), 3.15–3.06 (m, 2H), 2.93–2.85 (m, 2H), 2.62–2.56 (m, 2H), 1.06 (t, J = 7.2, 3H).

**1-Ethyl-3-(4-(7-(methylsulfonyl)-4-morpholino-5,6,7,8-tetrahydropyrido[3,4-d]pyrimidin-2-yl)phenyl)urea (12c)**. LC/MS (ESI): M<sup>+</sup> = 461, MW = 460.55. <sup>1</sup>H NMR (DMSO-*d*<sub>6</sub>, 400 MHz): δ 9.01 (s, 1H), 8.18 (d, J = 8.8, 2H), 7.49 (d, J = 8.8, 2H), 6.43 (s, 1H), 4.32 (s, 2H), 3.72 (s, 4H), 3.49 (d, J = 4.0 Hz, 4H), 3.12 (t, J = 6.4 Hz, 2H), 3.01 (s, 3H), 2.79 (s, 2H), 2.53 (s, 1H), 2.31 (s, 1H), 1.06 (t, J = 7.2 Hz, 3H). The purity of this compound was 87% by UV at 254 nm.

**Methyl 2-(4-(3-Ethylureido)phenyl)-4-morpholino-5,6-dihydropyrido[3,4-d]pyrimidine-7(8H)-carboxylate (12d)**. LC/MS (ESI): M<sup>+</sup> = 441, MW = 440.5. <sup>1</sup>H NMR (DMSO-*d*<sub>6</sub>, 400 MHz): δ 8.75 (s, 1H), 8.17 (d, J = 8.4 Hz, 2H), 7.51 (d, J = 8.4 Hz, 2H), 6.22 (s, 1H), 4.53 (s, 2H), 3.72–3.55 (m, 13H), 3.12 (t, J = 5.2 Hz, 2H), 2.69 (t, J = 5.2 Hz, 2H), 1.07 (t, J = 7.2 Hz, 3H). The purity of this compound was 94% by UV at 254 nm.

**1-(4-(7-Benzoyl-4-morpholino-5,6,7,8-tetrahydropyrido[3,4-d]pyrimidin-2-yl)phenyl)-3-ethylurea (12e)**. **12a** (111.6 mg, 0.2918 mmol) was weighed into a reaction vial. CH<sub>2</sub>Cl<sub>2</sub> (5.0 mL, 78 mmol) and *N,N*-diisopropylethylamine (150 μL, 0.86 mmol) were added and then benzoyl chloride (45 μL, 0.39 mmol). The reaction was stirred at rt for 2 h, and then the reaction was diluted with 8 mL of CH<sub>2</sub>Cl<sub>2</sub> and shaken with 10 mL of 1 N HCl. The layers were separated and then extracted with CH<sub>2</sub>Cl<sub>2</sub> (2 × 5 mL). The combined organic extracts were dried with MgSO<sub>4</sub>, filtered, and concentrated. The resulting material was purified by reverse-phase chromatography. LC/MS: 4.11 min, M<sup>+</sup> = 487.2, MW = 486.6. <sup>1</sup>H NMR (400 MHz, DMSO-*d*<sub>6</sub>): δ 10.12–9.97 (m, J = 23.6, 2H), 9.35 (s, 1H), 9.09 (s, 1H), 7.62 (d, J = 9.0, 1H), 6.97 (d, J = 8.7, 2H), 5.69 (s, 1H), 3.40–3.24 (m, J = 6.3, 13.6, 7H), 3.17 (s, 1H), 3.04–2.91 (m, 1H), 1.20 (t, J = 7.2, 3H), 0.97 (t, J = 7.2, 2H).

**Ethyl 4-(7-Benzoyl-4-morpholino-5,6,7,8-tetrahydropyrido[3,4-d]pyrimidin-2-yl)phenyl)carbamate (12f)**. LC/MS: 4.68 min, M<sup>+</sup> = 488.3, MW = 486.6. <sup>1</sup>H NMR (DMSO-*d*<sub>6</sub>, 400 MHz): δ 9.80 (s, 1H), 8.31–8.10 (m, 2H), 7.62–7.45 (m, 6H), 4.72 (br s, 1H), 4.53 (br s, 1H), 4.14 (q, J = 7.1 Hz, 2H), 3.83 (br s, 1H), 3.78–3.68 (m, 4H), 3.57–3.45 (m, 5H), 2.77 (t, J = 5.0 Hz, 2H), 1.26 (t, J = 7.1 Hz, 3H).

**4-(7-Benzoyl-4-morpholino-5,6,7,8-tetrahydropyrido[3,4-d]pyrimidin-2-yl)phenyl Ethylcarbamate (12g)**. LC/MS: 5.45 min, M<sup>+</sup> = 488.3, MW = 487.6. <sup>1</sup>H NMR (DMSO-*d*<sub>6</sub>, 400 MHz): δ 3.79–3.69 (m, 4H), 3.59–3.44 (m, 5H), 3.11 (p, J = 6.6 Hz, 2H), 2.78 (t, J = 5.1 Hz, 2H), 1.10 (t, J = 7.2 Hz, 3H), 3.91–3.79 (m, 1H), 8.43–8.15 (m, 2H), 7.82–7.73 (m, 1H), 7.57–7.46 (m, 4H), 7.26–7.09 (m, 2H), 4.80–4.47 (m, 2H).

**1-Ethyl-3-(4-(4-morpholino-7-(pyrimidin-2-yl)-5,6,7,8-tetrahydropyrido[3,4-d]pyrimidin-2-yl)phenyl)urea (12h)**. LC/MS: 3.97 min, M<sup>+</sup> = 461.2, MW = 460.5. <sup>1</sup>H NMR (DMSO-*d*<sub>6</sub>, 400 MHz): δ 8.64 (s, 1H), 8.43 (d, J = 4.7, 2H), 8.21 (d, J = 8.7, 2H), 7.49 (d, J = 8.8, 2H), 6.69 (t, J = 4.7, 1H), 6.16 (t, J = 5.5, 1H), 4.81 (s, 2H), 3.98 (s, 2H), 3.73 (d, J = 4.5, 4H), 3.47 (d, J = 4.4, 4H), 3.19–3.02 (m, 2H), 2.75 (s, 2H), 1.06 (t, J = 7.2, 3H).

**(S)-1-Ethyl-3-(4-(4-(3-methylmorpholino)-7-(pyrimidin-2-yl)-5,6,7,8-tetrahydropyrido[3,4-d]pyrimidin-2-yl)phenyl)urea (12i)**. LC/MS: 4.82 min, M<sup>+</sup> = 475.3, MW = 474.6. <sup>1</sup>H NMR (DMSO-*d*<sub>6</sub>, 400 MHz): δ 8.68 (s, 1H), 8.44 (d, J = 4.7, 2H), 8.20 (d, J = 8.8, 2H), 7.49 (d, J = 8.8, 2H), 6.69 (t, J = 4.7, 1H), 6.19 (t, J = 5.6, 1H), 4.90 (d, J = 18.7, 1H), 4.73 (d, J = 18.7, 1H), 4.19–4.06 (m, 2H), 3.94–3.76 (m, 2H), 3.74–3.54 (m, 4H), 3.50–3.36 (m, 1H), 3.17–

3.06 (m, 2H), 2.80–2.68 (m, 2H), 1.25 (d, J = 6.6, 3H), 1.06 (t, J = 7.2, 3H).

**(S)-1-Ethyl-3-(4-(4-(3-ethylmorpholino)-7-(pyrimidin-2-yl)-5,6,7,8-tetrahydropyrido[3,4-d]pyrimidin-2-yl)phenyl)urea (12j)**. LC/MS: 3.56 min, M<sup>+</sup> = 489.3, MW = 488.6. <sup>1</sup>H NMR (DMSO-*d*<sub>6</sub>, 400 MHz): δ 8.39 (d, J = 4.8 Hz, 2H), 8.30–8.16 (m, 2H), 7.50–7.38 (m, 2H), 6.70–6.55 (m, 1H), 5.06 (d, J = 18.7 Hz, 1H), 4.68 (d, J = 18.7 Hz, 1H), 4.39 (dt, J = 13.2, 4.8 Hz, 1H), 4.03 (s, 1H), 3.95–3.61 (m, 6H), 3.61–3.50 (m, 1H), 3.34 (s, 1H), 3.24 (d, J = 7.2 Hz, 1H), 2.94–2.62 (m, 2H), 1.90 (ddd, J = 13.8, 9.9, 6.7 Hz, 2H), 1.17 (t, J = 7.2 Hz, 3H), 0.98–0.80 (m, 3H).

**(S)-1-ethyl-3-(4-(4-(3-methylmorpholino)-7-(pyrazin-2-yl)-5,6,7,8-tetrahydropyrido[3,4-d]pyrimidin-2-yl)phenyl)urea (12k)**. LC/MS: 3.05 min, M<sup>+</sup> = 475.2, MW = 474.6. <sup>1</sup>H NMR (DMSO-*d*<sub>6</sub>, 400 MHz): δ 8.67 (s, 1H), 8.43 (d, J = 1.5 Hz, 1H), 8.24–8.16 (m, 2H), 8.13 (dd, J = 2.6, 1.5 Hz, 1H), 7.87 (d, J = 2.6 Hz, 1H), 7.55–7.44 (m, 2H), 6.19 (t, J = 5.5 Hz, 1H), 4.87–4.49 (m, 2H), 4.14 (d, J = 7.4 Hz, 1H), 3.99 (dt, J = 12.8, 5.0 Hz, 1H), 3.94–3.82 (m, 1H), 3.82–3.52 (m, 5H), 3.51–3.37 (m, 1H), 3.12 (dt, J = 12.7, 7.1 Hz, 2H), 2.78 (t, J = 5.5 Hz, 2H), 1.26 (d, J = 6.6 Hz, 3H), 1.06 (t, J = 7.2 Hz, 3H).

**(S)-1-Ethyl-3-(4-(4-(3-methylmorpholino)-7-(pyridazin-3-yl)-5,6,7,8-tetrahydropyrido[3,4-d]pyrimidin-2-yl)phenyl)urea (12l)**. LC/MS: 3.63 min, M<sup>+</sup> = 475.2, MW = 474.6. <sup>1</sup>H NMR (DMSO-*d*<sub>6</sub>, 400 MHz): δ 8.66 (s, 1H), 8.58 (dd, J = 4.3, 1.3 Hz, 1H), 8.21 (d, J = 8.8 Hz, 2H), 7.50 (d, J = 8.8 Hz, 2H), 7.46–7.36 (m, 2H), 6.17 (t, J = 5.6 Hz, 1H), 4.78 (d, J = 18.1 Hz, 1H), 4.66 (d, J = 18.1 Hz, 1H), 4.17–4.00 (m, 2H), 3.93–3.84 (m, 1H), 3.82–3.56 (m, 5H), 3.48–3.39 (m, 1H), 3.17–3.07 (m, 2H), 2.83–2.75 (m, 2H), 1.26 (d, J = 6.7 Hz, 3H), 1.06 (t, J = 7.2 Hz, 3H). The purity of this compound was 89% by UV at 254 nm.

**(S)-1-Ethyl-3-(4-(7-(3-methyl-1,2,4-thiadiazol-5-yl)-4-(3-methylmorpholino)-5,6,7,8-tetrahydropyrido[3,4-d]pyrimidin-2-yl)phenyl)urea (12m)**. LC/MS: 3.58 min, M<sup>+</sup> = 495.2, MW = 494.6. <sup>1</sup>H NMR (DMSO-*d*<sub>6</sub>, 400 MHz): δ 8.78 (s, 1H), 8.19 (d, J = 8.8 Hz, 2H), 7.50 (d, J = 8.8 Hz, 2H), 6.29 (t, J = 5.7 Hz, 1H), 4.59 (d, J = 4.8 Hz, 2H), 4.14–4.08 (m, 2H), 3.90–3.58 (m, 5H), 3.47–3.42 (m, 1H), 3.15–3.08 (m, 2H), 2.85–2.81 (m, 2H), 2.69–2.66 (m, 1H), 2.33 (s, 3H), 1.26 (d, i = 6.7 Hz, 3H), 1.06 (t, J = 7.2 Hz, 3H).

**(S)-1-Ethyl-3-(4-(7-(5-methyl-1,3,4-oxadiazol-2-yl)-4-(3-methylmorpholino)-5,6,7,8-tetrahydropyrido[3,4-d]pyrimidin-2-yl)phenyl)urea (12n)**. LC/MS (ESI): M<sup>+</sup> = 479.3, MW = 478.55. <sup>1</sup>H NMR (DMSO-*d*<sub>6</sub>, 400 MHz): δ 8.73 (s, 1H), 8.09 (d, J = 8.8 Hz, 2H), 7.45 (d, J = 8.8 Hz, 2H), 6.20 (s, 1H), 4.51 (s, 1H), 4.25 (s, 1H), 3.59–3.44 (m, 8H), 3.05 (d, J = 5.6 Hz, 2H), 2.29 (s, 3H), 1.23 (d, J = 6.4 Hz, 3H), 0.99 (t, J = 7.2 Hz, 3H).

**Molecular Modeling.** A homology model of the mTOR kinase domain was built from publicly available PI3Kγ crystal structures (PDB code 3IBE) using the Fugue and Orchestrate modules of Sybyl, version 8.1 (Tripos Associates, St. Louis, MO), and further optimized using the Maximin module within Sybyl (all atoms, Amber FF02 charges on protein, MMFF94 charges on ligand) including the bound ligand from 3IBE. Docking studies were conducted using Gold, version 4.1, with a single hydrogen bond constraint to the hinge Val backbone NH, allowing flexible Lys and Asp side chains so appropriate hydrogen bond geometry between the ligand urea moiety and protein could be attained. A 10 Å sphere around the centroid of the ligand was used to define the active site region.

## AUTHOR INFORMATION

### Corresponding Author

\*Phone: 650-225-1000. Fax: 650-467-8922. E-mail: mkoehler@gene.com.

### Notes

The authors declare the following competing financial interests: M.F.T.K. is an employee of Genentech, Inc. and a stockholder of F. Hoffman-La Roche Ltd.

## ACKNOWLEDGMENTS

We thank members of the DMPK and Purification groups within Genentech Small Molecule Drug Discovery for analytical support.

## ABBREVIATIONS USED

mTOR, mammalian target of rapamycin; PI3K, phosphatidylinositol 3 kinase; mTORC, mammalian target of rapamycin complex; LC/MS, liquid chromatography–mass spectrometry; TPSA, topological polar surface area; PPB, plasma protein binding; PTEN, phosphatase and tensin homologue; CYP, cytochrome P450.

## REFERENCES

(1) Baselga, J.; Campone, M.; Piccart, M.; Burris, H. A., III; Rugo, H. S.; Sahnoud, T.; Noguchi, S.; Gnant, M.; Pritchard, K. I.; Lebrun, F.; Beck, J. T.; Ito, Y.; Yardley, D.; Deleu, I.; Perez, A.; Bachelot, T.; Vittori, L.; Xu, Z.; Mukhopadhyay, P.; Lebewohl, D.; Hortobagyi, G. N. Everolimus in Postmenopausal Hormone-Receptor-Positive Advanced Breast Cancer. *N. Engl. J. Med.* **2011**, *366*, 520–529.

(2) Sabatini, D. M. mTOR and cancer: Insights into a complex relationship. *Nat. Rev. Cancer* **2006**, *6*, 729–734.

(3) Liu, K. K. C.; Bailey, S.; Dinh, D. M.; Lam, H.; Li, C.; Wells, P. A.; Yin, M.-J.; Zou, A. Conformationally-restricted cyclic sulfones as potent and selective mTOR kinase inhibitors. *Bioorg. Med. Chem. Lett.* **2012**, *22*, 5114–5117.

(4) Peterson, E. A.; Boezio, A. A.; Andrews, P. S.; Boezio, C. M.; Bush, T. L.; Cheng, A. C.; Choquette, D.; Coats, J. R.; Colletti, A. E.; Copeland, K. W.; DuPont, M.; Graceffa, R.; Grubinska, B.; Kim, J. L.; Lewis, R. T.; Liu, J.; Mullady, E. L.; Potashman, M. H.; Romero, K.; Shaffer, P. L.; Stanton, M. K.; Stellwagen, J. C.; Teffera, Y.; Yi, S.; Cai, T.; La, D. S. Discovery and optimization of potent and selective imidazopyridine and imidazopyridazine mTOR inhibitors. *Bioorg. Med. Chem. Lett.* **2012**, *22*, 4967–4974.

(5) Finlay, M. R. V.; Buttar, D.; Critchlow, S. E.; Dishington, A. P.; Fillery, S. M.; Fisher, E.; Glossop, S. C.; Graham, M. A.; Johnson, T.; Lamont, G. M.; Mutton, S.; Perkins, P.; Pike, K. G.; Slater, A. M. Sulfonyl-morpholino-pyrimidines: SAR and development of a novel class of selective mTOR kinase inhibitor. *Bioorg. Med. Chem. Lett.* **2012**, *22*, 4163–4168.

(6) Mortensen, D. S.; Perrin-Ninkovic, S. M.; Harris, R.; Lee, B. G. S.; Shevlin, G.; Hickman, M.; Khambatta, G.; Bisonette, R. R.; Fultz, K. E.; Sankar, S. Discovery and SAR exploration of a novel series of imidazo[4,5-*b*]pyrazin-2-ones as potent and selective mTOR kinase inhibitors. *Bioorg. Med. Chem. Lett.* **2011**, *21*, 6793–6799.

(7) Bhagwat, S. V.; Gokhale, P. C.; Crew, A. P.; Cooke, A.; Yao, Y.; Mantis, C.; Kahler, J.; Workman, J.; Bittner, M.; Dudkin, L.; Epstein, D. M.; Gibson, N. W.; Wild, R.; Arnold, L. D.; Houghton, P. J.; Pachter, J. A. Preclinical Characterization of OSI-027, a Potent and Selective Inhibitor of mTORC1 and mTORC2: Distinct from Rapamycin. *Mol. Cancer Ther.* **2011**, *10*, 1394–1406.

(8) Liu, Q.; Wang, J.; Kang, S. A.; Thoreen, C. C.; Hur, W.; Choi, H. G.; Waller, D. L.; Sim, T.; Sabatini, D. M.; Gray, N. S. Discovery and optimization of potent and selective benzonaphthyridinone analogs as small molecule mTOR inhibitors with improved mouse microsome stability. *Bioorg. Med. Chem. Lett.* **2011**, *21*, 4036–4040.

(9) Cohen, F.; Bergeron, P.; Blackwood, E.; Bowman, K. K.; Chen, H.; Dipasquale, A. G.; Epler, J. A.; Koehler, M. F. T.; Lau, K.; Lewis, C.; Liu, L.; Ly, C. Q.; Malek, S.; Nonomiya, J.; Ortwine, D. F.; Pei, Z.; Robarge, K. D.; Sideris, S.; Trinh, L.; Truong, T.; Wu, J.; Zhao, X.; Lyssikatos, J. P. Potent, selective, and orally bioavailable inhibitors of mammalian target of rapamycin (mTOR) kinase based on a quaternary substituted dihydrofuropyrimidine. *J. Med. Chem.* **2011**, *54*, 3426–3435.

(10) Crew, A. P.; Bhagwat, S. V.; Dong, H.; Bittner, M. A.; Chan, A.; Chen, X.; Coate, H.; Cooke, A.; Gokhale, P. C.; Honda, A.; Jin, M.; Kahler, J.; Mantis, C.; Mulvihill, M. J.; Tavares-Greco, P. A.; Volk, B.;

Wang, J.; Werner, D. S.; Arnold, L. D.; Pachter, J. A.; Wild, R.; Gibson, N. W. Imidazo[1,5-*a*]pyrazines: Orally efficacious inhibitors of mTORC1 and mTORC2. *Bioorg. Med. Chem. Lett.* **2011**, *21*, 2092–2097.

(11) Peterson, E. A.; Andrews, P. S.; Be, X.; Boezio, A. A.; Bush, T. L.; Cheng, A. C.; Coats, J. R.; Colletti, A. E.; Copeland, K. W.; DuPont, M.; Graceffa, R.; Grubinska, B.; Harmange, J.-C.; Kim, J. L.; Mullady, E. L.; Olivieri, P.; Schenkel, L. B.; Stanton, M. K.; Teffera, Y.; Whittington, D. A.; Cai, T.; La, D. S. Discovery of triazine-benzimidazoles as selective inhibitors of mTOR. *Bioorg. Med. Chem. Lett.* **2011**, *21*, 2064–2070.

(12) Liu, Q.; Wang, J.; Kang, S. A.; Thoreen, C. C.; Hur, W.; Ahmed, T.; Sabatini, D. M.; Gray, N. S. Discovery of 9-(6-aminopyridin-3-yl)-1-(3-(trifluoromethyl)phenyl)benzo[*h*][1,6]naphthyridin-2(1*H*)-one (Torin2) as a potent, selective, and orally available mammalian target of rapamycin (mTOR) inhibitor for treatment of cancer. *J. Med. Chem.* **2011**, *54*, 1473–1480.

(13) Liu, Q.; Chang, J. W.; Wang, J.; Kang, S. A.; Thoreen, C. C.; Markhard, A.; Hur, W.; Zhang, J.; Sim, T.; Sabatini, D. M.; Gray, N. S. Discovery of 1-(4-(4-propionylpiperazin-1-yl)-3-(trifluoromethyl)phenyl)-9-(quinolin-3-yl)benzo[*h*][1,6]naphthyridin-2(1*H*)-one as a highly potent, selective mammalian target of rapamycin (mTOR) inhibitor for the treatment of cancer. *J. Med. Chem.* **2010**, *53*, 7146–7155.

(14) Richard, D. J.; Verheijen, J. C.; Yu, K.; Zask, A. Triazines incorporating (*R*)-3-methylmorpholine are potent inhibitors of the mammalian target of rapamycin (mTOR) with selectivity over PI3Kalpha. *Bioorg. Med. Chem. Lett.* **2010**, *20*, 2654–2657.

(15) Zask, A.; Verheijen, J. C.; Richard, D. J.; Kaplan, J.; Curran, K.; Toral-Barza, L.; Lucas, J.; Hollander, I.; Yu, K. Discovery of 2-ureidophenyltriazines bearing bridged morpholines as potent and selective ATP-competitive mTOR inhibitors. *Bioorg. Med. Chem. Lett.* **2010**, *20*, 2644–2647.

(16) Tsou, H.-R.; MacEwan, G.; Birnberg, G.; Zhang, N.; Brooijmans, N.; Toral-Barza, L.; Hollander, I.; Ayril-Kaloustian, S.; Yu, K. 4-Substituted-7-azaindoles bearing a ureidobenzofuranone moiety as potent and selective, ATP-competitive inhibitors of the mammalian target of rapamycin (mTOR). *Bioorg. Med. Chem. Lett.* **2010**, *20*, 2259–2263.

(17) Curran, K. J.; Verheijen, J. C.; Kaplan, J.; Richard, D. J.; Toral-Barza, L.; Hollander, I.; Lucas, J.; Ayril-Kaloustian, S.; Yu, K.; Zask, A. Pyrazolopyrimidines as highly potent and selective, ATP-competitive inhibitors of the mammalian target of rapamycin (mTOR): Optimization of the 1-substituent. *Bioorg. Med. Chem. Lett.* **2010**, *20*, 1440–1444.

(18) Kaplan, J.; Verheijen, J. C.; Brooijmans, N.; Toral-Barza, L.; Hollander, I.; Yu, K.; Zask, A. Discovery of 3,6-dihydro-2*H*-pyran as a morpholine replacement in 6-aryl-1*H*-pyrazolo[3,4-*d*]pyrimidines and 2-arylthieno[3,2-*d*]pyrimidines: ATP-competitive inhibitors of the mammalian target of rapamycin (mTOR). *Bioorg. Med. Chem. Lett.* **2010**, *20*, 640–643.

(19) Chresta, C. M.; Davies, B. R.; Hickson, I.; Harding, T.; Cosulich, S.; Critchlow, S. E.; Vincent, J. P.; Ellston, R.; Jones, D.; Sini, P.; James, D.; Howard, Z.; Dudley, P.; Hughes, G.; Smith, L.; Maguire, S.; Hummersone, M.; Malagu, K.; Menear, K.; Jenkins, R.; Jacobsen, M.; Smith, G. C. M.; Guichard, S.; Pass, M. AZD8055 is a potent, selective, and orally bioavailable ATP-competitive mammalian target of rapamycin kinase inhibitor with in vitro and in vivo antitumor activity. *Cancer Res.* **2010**, *70*, 288–298.

(20) Verheijen, J. C.; Yu, K.; Toral-Barza, L.; Hollander, I.; Zask, A. Discovery of 2-arylthieno[3,2-*d*]pyrimidines containing 8-oxa-3-azabicyclo[3.2.1]octane in the 4-position as potent inhibitors of mTOR with selectivity over PI3K. *Bioorg. Med. Chem. Lett.* **2010**, *20*, 375–379.

(21) Zask, A.; Kaplan, J.; Verheijen, J. C.; Richard, D. J.; Curran, K.; Brooijmans, N.; Bennett, E. M.; Toral-Barza, L.; Hollander, I.; Ayril-Kaloustian, S.; Yu, K. Morpholine derivatives greatly enhance the selectivity of mammalian target of rapamycin (mTOR) inhibitors. *J. Med. Chem.* **2009**, *52*, 7942–7945.

- (22) Nowak, P.; Cole, D. C.; Brooijmans, N.; Bursavich, M. G.; Curran, K. J.; Ellingboe, J. W.; Gibbons, J. J.; Hollander, I.; Hu, Y.; Kaplan, J.; Malwitz, D. J.; Toral-Barza, L.; Verheijen, J. C.; Zask, A.; Zhang, W.-G.; Yu, K. Discovery of potent and selective inhibitors of the mammalian target of rapamycin (mTOR) kinase. *J. Med. Chem.* **2009**, *52*, 7081–7089.
- (23) Malagu, K.; Duggan, H.; Menear, K.; Hummersone, M.; Gomez, S.; Bailey, C.; Edwards, P.; Drzewiecki, J.; Leroux, F.; Quesada, M. J. The discovery and optimization of pyrido[2,3-*d*]pyrimidine-2,4-diamines as potent and selective inhibitors of mTOR kinase. *Bioorg. Med. Chem. Lett.* **2009**, *19*, S950–S953.
- (24) Menear, K. A.; Gomez, S.; Malagu, K.; Bailey, C.; Blackburn, K.; Cockcroft, X.-L.; Ewen, S.; Fundo, A.; Gall, A. L.; Hermann, G. Identification and optimization of novel and selective small molecular weight kinase inhibitors of mTOR. *Bioorg. Med. Chem. Lett.* **2009**, *19*, 5898–5901.
- (25) Zask, A.; Verheijen, J. C.; Curran, K.; Kaplan, J.; Richard, D. J.; Nowak, P.; Malwitz, D. J.; Brooijmans, N.; Bard, J.; Svenson, K.; Lucas, J.; Toral-Barza, L.; Zhang, W.-G.; Hollander, I.; Gibbons, J. J.; Abraham, R. T.; Ayril-Kaloustian, S.; Mansour, T. S.; Yu, K. ATP-competitive inhibitors of the mammalian target of rapamycin: Design and synthesis of highly potent and selective pyrazolopyrimidines. *J. Med. Chem.* **2009**, *52*, 5013–5016.
- (26) Yu, K.; Toral-Barza, L.; Shi, C.; Zhang, W.-G.; Lucas, J.; Shor, B.; Kim, J.; Verheijen, J.; Curran, K.; Malwitz, D. J.; Cole, D. C.; Ellingboe, J.; Ayril-Kaloustian, S.; Mansour, T. S.; Gibbons, J. J.; Abraham, R. T.; Nowak, P.; Zask, A. Biochemical, cellular, and in vivo activity of novel ATP-competitive and selective inhibitors of the mammalian target of rapamycin. *Cancer Res.* **2009**, *69*, 6232–6240.
- (27) García Martínez, J. M.; Moran, J.; Clarke, R. G.; Gray, A.; Cosulich, S. C.; Chresta, C. M.; Alessi, D. R. Ku-0063794 is a specific inhibitor of the mammalian target of rapamycin (mTOR). *Biochem. J.* **2009**, *421*, 29–42.
- (28) Feldman, M. E.; Apsel, B.; Uotila, A.; Loewith, R.; Knight, Z. A.; Ruggero, D.; Shokat, K. M. Active-site inhibitors of mTOR target rapamycin-resistant outputs of mTORC1 and mTORC2. *Plos Biol.* **2009**, *7*, e38.
- (29) Folkes, A. J.; Ahmadi, K.; Alderton, W. K.; Alix, S.; Baker, S. J.; Box, G.; Chuckowree, I. S.; Clarke, P. A.; Depledge, P.; Eccles, S. A.; Friedman, L. S.; Hayes, A.; Hancox, T. C.; Kugendradas, A.; Lensun, L.; Moore, P.; Olivero, A. G.; Pang, J.; Patel, S.; Pergl-Wilson, G. H.; Raynaud, F. I.; Robson, A.; Saghir, N.; Salphati, L.; Sohal, S.; Ultsch, M. H.; Valenti, M.; Wallweber, H. J. A.; Wan, N. C.; Wiesmann, C.; Workman, P.; Zhyvoloup, A.; Zvelebil, M. J.; Shuttleworth, S. J. The identification of 2-(1*H*-indazol-4-yl)-6-(4-methanesulfonyl-piperazin-1-ylmethyl)-4-morpholin-4-yl-thieno[3,2-*d*]pyrimidine (GDC-0941) as a potent, selective, orally bioavailable inhibitor of class I PI3 kinase for the treatment of cancer. *J. Med. Chem.* **2008**, *51*, 5522–5532.
- (30) Sutherlin, D. P.; Bao, L.; Berry, M.; Castanedo, G.; Chuckowree, I.; Dotson, J.; Folks, A.; Friedman, L.; Goldsmith, R.; Gunzner, J.; Heffron, T.; Lesnick, J.; Lewis, C.; Mathieu, S.; Murray, J.; Nonomiya, J.; Pang, J.; Pegg, N.; Prior, W. W.; Rouge, L.; Salphati, L.; Sampath, D.; Tian, Q.; Tsui, V.; Wan, N. C.; Wang, S.; Wei, B.; Wiesmann, C.; Wu, P.; Zhu, B.-Y.; Olivero, A. Discovery of a potent, selective, and orally available class I phosphatidylinositol 3-kinase (PI3K)/mammalian target of rapamycin (mTOR) kinase inhibitor (GDC-0980) for the treatment of cancer. *J. Med. Chem.* **2011**, *54*, 7579–7587.
- (31) Sutherlin, D. P.; Sampath, D.; Berry, M.; Castanedo, G.; Chang, Z.; Chuckowree, I.; Dotson, J.; Folkes, A.; Friedman, L.; Goldsmith, R.; Heffron, T.; Lee, L.; Lesnick, J.; Lewis, C.; Mathieu, S.; Nonomiya, J.; Olivero, A.; Pang, J.; Prior, W. W.; Salphati, L.; Sideris, S.; Tian, Q.; Tsui, V.; Wan, N. C.; Wang, S.; Wiesmann, C.; Wong, S.; Zhu, B.-Y. Discovery of (thienopyrimidin-2-yl)aminopyrimidines as potent, selective, and orally available pan-PI3-kinase and dual pan-PI3-kinase/mTOR inhibitors for the treatment of cancer. *J. Med. Chem.* **2010**, *53*, 1086–1097.
- (32) Yang, B. V.; O'Rourke, D.; Li, J. Mild and selective debenzoylation of tertiary amines using  $\alpha$ -chloroethyl chloroformate. *Synlett* **1993**, *1993*, 195–196.
- (33) Leach, A. G.; Jones, H. D.; Cosgrove, D. A.; Kenny, P. W.; Ruston, L.; MacFaul, P.; Wood, J. M.; Colclough, N.; Law, B. Matched molecular pairs as a guide in the optimization of pharmaceutical properties; a study of aqueous solubility, plasma protein binding and oral exposure. *J. Med. Chem.* **2006**, *49*, 6672–6682.
- (34) Grünwald, V.; DeGraffenried, L.; Russel, D.; Friedrichs, W. E.; Ray, R. B.; Hidalgo, M. Inhibitors of mTOR reverse doxorubicin resistance conferred by PTEN status in prostate cancer cells. *Cancer Res.* **2002**, *62*, 6141–6145.
- (35) Halladay, J. S.; Delarosa, E. M.; Tran, D.; Wang, L.; Wong, S.; Khojasteh, S. C. High-throughput, 384-well, LC–MS/MS CYP inhibition assay using automation, cassette-analysis technique, and streamlined data analysis. *Drug Metab. Lett.* **2011**, *5*, 220–230.
- (36) Wallin, J. J.; Edgar, K. A.; Guan, J.; Berry, M.; Prior, W. W.; Lee, L.; Lesnick, J. D.; Lewis, C.; Nonomiya, J.; Pang, J.; Salphati, L.; Olivero, A. G.; Sutherlin, D. P.; O'Brien, C.; Spoerke, J. M.; Patel, S.; Lensun, L.; Kassees, R.; Ross, L.; Lackner, M. R.; Sampath, D.; Belvin, M.; Friedman, L. S. GDC-0980 is a novel class I PI3K/mTOR kinase inhibitor with robust activity in cancer models driven by the PI3K pathway. *Mol. Cancer Ther.* **2011**, *10*, 2426–2436.
- (37) Hidalgo, M.; Buckner, J. C.; Erlichman, C.; Pollack, M. S.; Boni, J. P.; Dukart, G.; Marshall, B.; Speicher, L.; Moore, L.; Rowinsky, E. K. A phase I and pharmacokinetic study of temsirolimus (CCI-779) administered intravenously daily for 5 days every 2 weeks to patients with advanced cancer. *Clin. Cancer Res.* **2006**, *12*, 5755–5763.
- (38) Cloughesy, T.; Yoshimoto, K.; Nghiemphu, P. Antitumor activity of rapamycin in a phase I trial for patients with recurrent PTEN-deficient glioblastoma. *PLoS Med.* **2008**, *5*, e8.
- (39) Taberner, J.; Rojo, F.; Calvo, E.; Burris, H.; Judson, I.; Hazell, K.; Martinelli, E.; Cajal, S. R. Y.; Jones, S.; Vidal, L.; Shand, N.; Macarulla, T.; Ramos, F. J.; Dimitrijevic, S.; Zoellner, U.; Tang, P.; Stumm, M.; Lane, H. A.; Lebowohl, D.; Baselga, J. Dose- and schedule-dependent inhibition of the mammalian target of rapamycin pathway with everolimus: A phase I tumor pharmacodynamic study in patients with advanced solid tumors. *J. Clin. Oncol.* **2008**, *26*, 1603–1610.